UNIVERSIDAD DE INVESTIGACIÓN DE TECNOLOGÍA EXPERIMENTAL YACHAY TECH

Escuela de Ciencias de la Tierra Energía y Ambiente

Thermal and Morphological Changes of the

Volcán de Colima Lava Dome 2013 – 2016.

Trabajo de titulación presentado como requisito para la obtención del título de Geóloga.

Autor:

ANDREA BELEN TONATO ÑACATO

Tutor:

PhD. CELINE LUCIE MANDON

Urcuquí, marzo 2020

SECRETARÍA GENERAL
(Vicerrectorado Académico/Cancillería)
ESCUELA DE CIENCIAS DE LA TIERRA, ENERGÍA Y AMBIENTE
CARRERA DE GEOLOGÍA
ACTA DE DEFENSA No. UITEY-GEO-2020-00006-AD

A los 8 días del mes de abril de 2020, a las 10:00 horas, de manera virtual mediante videoconferencia, y ante el Tribunal Calificador, integrado por los docentes:

Presidente Tribunal de Defensa	Dra. FOSTER ANNA ELIZABETH , Ph.D.
Miembro No Tutor	Dra. PIISPA , ELISA JOHANNA , Ph.D.
Tutor	Dra. MANDON CELINE LUCIE , Ph.D.

El(la) señor(ita) estudiante TONATO ÑACATO, ANDREA BELEN, con cédula de identidad No. 1722908017, de la ESCUELA DE CIENCIAS DE LA TIERRA, ENERGÍA Y AMBIENTE, de la Carrera de GEOLOGÍA, aprobada por el Consejo de Educación Superior (CES), mediante Resolución RPC-SE-10-No.031-2016, realiza a través de videoconferencia, la sustentación de su trabajo de titulación denominado: THERMAL AND MORPHOLOGICAL CHANGES OF THE VOLCÁN DE COLIMA LAVA DOME 2013 – 2016, previa a la obtención del título de GEÓLOGO/A.

El citado trabajo de titulación, fue debidamente aprobado por el(los) docente(s):

Tutor	Dra. MANDON CELINE LUCIE , Ph.D.

Y recibió las observaciones de los otros miembros del Tribunal Calificador, las mismas que han sido incorporadas por el(la) estudiante.

Previamente cumplidos los requisitos legales y reglamentarios, el trabajo de titulación fue sustentado por el(la) estudiante y examinado por los miembros del Tribunal Calificador. Escuchada la sustentación del trabajo de titulación a través de videoconferencia, que integró la exposición de el(la) estudiante sobre el contenido de la misma y las preguntas formuladas por los miembros del Tribunal, se califica la sustentación del trabajo de titulación con las siguientes calificaciones:

Tipo	Docente	Calificación
Miembro Tribunal De Defensa	Dra. PIISPA , ELISA JOHANNA , Ph.D.	9,4
Tutor	Dra. MANDON CELINE LUCIE , Ph.D.	9,3
Presidente Tribunal De Defensa	Dra. FOSTER ANNA ELIZABETH , Ph.D.	9,5

Lo que da un promedio de: 9.4 (Nueve punto Cuatro), sobre 10 (diez), equivalente a: APROBADO

Para constancia de lo actuado, firman los miembros del Tribunal Calificador, el/la estudiante y el/la secretario ad-hoc.

Certifico que *en cumplimiento del Decreto Ejecutivo 1017 de 16 de marzo de 2020, la defensa de trabajo de titulación (o examen de grado modalidad teórico práctica) se realizó vía virtual, por lo que las firmas de los miembros del Tribunal de Defensa de Grado, constan en forma digital.*

TONATO ÑACATO, ANDREA BELEN
Estudiante

Dra. FOSTER ANNA ELIZABETH , Ph.D.
Presidente Tribunal de Defensa

ANNA ELIZABETH FOSTER
Digitally signed by ANNA ELIZABETH FOSTER
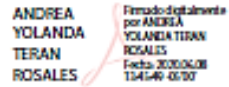Date: 2020.04.08 17:45:27 -05'00'

Dra. MANDON CELINE LUCIE , Ph.D.
Tutor

CELINE LUCIE

Dra. PIISPA , ELISA JOHANNA , Ph.D.
Miembro No Tutor

TERÁN ROSALES, ANDREA YOLANDA
Secretario Ad-hoc

AUTORÍA

Yo, **Andrea Belen Tonato Ñacato**, con cédula de identidad **1722908017**, declaro que las ideas, juicios, valoraciones, interpretaciones, consultas bibliográficas, definiciones y conceptualizaciones expuestas en el presente trabajo; así cómo, los procedimientos y herramientas utilizadas en la investigación, son de absoluta responsabilidad de la autora del trabajo de integración curricular. Así mismo, me acojo a los reglamentos internos de la Universidad de Investigación de Tecnología Experimental Yachay.

Urcuquí, julio 2020

_____

Andrea Belen Tonato Ñacato

CI: 1722908017

AUTORIZACIÓN DE PUBLICACIÓN

Yo, **Andrea Belen Tonato Ñacato,** con cédula de identidad **1722908017**, cedo a la Universidad de Investigación de Tecnología Experimental Yachay, los derechos de publicación de la presente obra, sin que deba haber un reconocimiento económico por este concepto. Declaro además que el texto del presente trabajo de titulación no podrá ser cedido a ninguna empresa editorial para su publicación u otros fines, sin contar previamente con la autorización escrita de la Universidad.

Asimismo, autorizo a la Universidad que realice la digitalización y publicación de este trabajo de integración curricular en el repositorio virtual, de conformidad a lo dispuesto en el Art. 144 de la Ley Orgánica de Educación Superior

Urcuquí, julio 2020.

_____
Andrea Belen Tonato Ñacato
CI: 1722908017

Acknowledgments

Andrea Belen Tonato Ñacato

Resumen

El Volcán Colima es uno de los volcanes más activos en América del Norte, perteneciente al sector occidental del Cinturón Volcánico Transmexicano. La actividad eruptiva histórica de Colima se ha caracterizado por una compleja sucesión de erupciones efusivas de domos de lava y/o flujos de lava asociados a flujos de bloques y cenizas, y erupciones explosivas de diversa magnitud que han producido numerosos y diversos tipos de flujos piroclásticos y caídas de tefra . Este proyecto de tesis analiza fotografías aéreas e imágenes térmicas de domos de lava en el Volcán de Colima de 2013 a 2016, junto con un estudio de las tasas de efusión para el crecimiento de un domo de lava en 2016. En base a los cambios morfológicos, definimos cuatro fases diferentes de actividad efusiva y explosiva del volcán durante todo el período de 2013 a 2016. Incluye fases de crecimiento, colapso y destrucción de un domo de lava acompañado de cambios en los procesos de crecimiento, temperaturas y texturas de lava. Los datos térmicos mostraron que durante el período 2013-2016, las temperaturas máximas observadas varían de 150ºC a 500ºC. La temperatura más alta se registró durante la última etapa del crecimiento del domo de lava de 2016, el 4 de octubre. Finalmente, las tasas de efusión calculadas para el crecimiento del domo de lava de 2016 indican un valor máximo de $\sim 3.08 \times 104 \ m^3 \ día^{-1}$. El crecimiento del domo de lava de 2016 se dividió en cuatro etapas según la velocidad de efusión, la temperatura, el tipo de material extruido y el proceso de crecimiento. Nuestros resultados proporcionan información importante sobre los procesos subyacentes del movimiento y el emplazamiento del magma a niveles poco profundos, así como una evaluación de riesgos y peligros.

Palabras clave: domo de lava, tasa de efusión, exógeno, endógeno, efusivo, explosivo.

Abstract

Volcán de Colima is one of the most active volcanoes in North America, belonging to the western sector of the Trans-Mexican Volcanic Belt. The historical eruptive activity of Colima has been characterized by a complex succession of effusive lava-dome and/or lava flow eruptions with associated block and ash flows, and explosive eruptions of varying magnitude that have produced numerous and diverse types of pyroclastic flows and tephra falls. This thesis project analyses aerial photographs and thermal images of lava domes at Volcán de Colima from 2013 to 2016 along with a study of effusion rates for a lava dome growth in 2016. Based on the morphological changes, we defined four different phases of effusive and explosive activity of the volcano during the whole period 2013-2016. It includes phases of growth, collapse and destruction of a lava dome accompanied by changes in growth processes, temperatures, and lava textures. Thermal data showed that during the period 2013-2016, the maximum observed temperatures vary from 150ºC to 500ºC. The highest temperature was recorded during the last stage of the 2016 lava dome growth, on 4th of October. Finally, effusion rates calculated for the 2016 lava dome growth indicate a maximum value of ~3.08×10^4 m^{3}days^{-1}. Growth of the 2016 lava dome was divided into four stages depending on the effusion rate, temperature, type of extruded material, and process of growth. Our results provide important information on the underlying processes of magma movement and emplacement at shallow levels, as well as an assessment of risk and hazard.

Key Words: lava dome, effusion rate, exogenous, endogenous, effusive, explosive.

Table of Contents

1. Introduction

Lava domes are volcanic features formed when viscous magma cools relatively quickly after emerging onto the surface. Similar to lava flows, they do not have enough pressure from gases to produce an explosive eruption. Despite that, effusive eruptions of lava domes can be preceded or followed by explosive activity. They themselves can generate rock falls, debris avalanches and pyroclastic flows due to their unstable structure. This stability can be affected by gravity, internal gas overpressure, intense rainfall, a switch in extrusion direction, topography under the dome, hydrothermal alteration, dome growth (dynamic or explosive) and tectonic faulting (Harnett et al., 2018). Lava domes are diverse in shapes and habits. Their morphology is principally controlled by magma rheology, substrate topography, ascent dynamics, and the mechanism of dome growth (Calder et al., 2015). There are two dome growth mechanisms: endogenous, in which the lava dome increases in size due to intrusion of new magma below its surface, and exogenous growth where the dome increases its size due to magma forcing its way to the surface, forming lobes of lava that pile on top of, or adjacent to each other (Fig. 1.1).
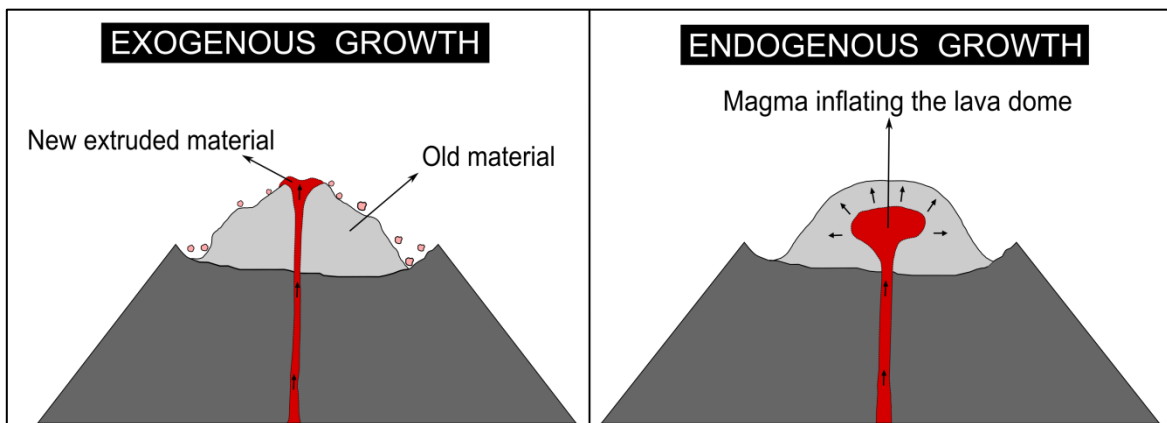

Fig. 1.1. *Sketch showing the difference between exogenous and endogenous growth of a lava dome.*

According to Fink (1990), a dome-building eruption is a type of volcanism which is very common in convergent margin settings, with domes forming in the crater of volcanic cones, or within a dome cluster or dome complex. The composition of lava forming domes can range from basaltic to rhyolitic, although most domes have intermediate composition

(andesitic and dacitic). Petrographically speaking, there are two types of lava domes: obsidian domes which are crystal-poor and rhyolitic to rhyodacitic in composition, and crystal-rich domes with a basaltic andesite composition (Calder et al., 2015).

Over the last three decades, the contribution of dome-building eruptions to the understanding of magma transport and eruptive styles has been extremely rich and important in the volcanology field (Calder et al., 2015). Some of the events that provided comprehensive data sets to create models of crystal-bearing magma ascent and lava dome eruption dynamics were Mount St. Helens, USA (1980 – 1986 and 2004 – 2008), Soufrière Hills, Montserrat (1995 – 2013), and Unzen in Japan (1990 – 1995). In particular, during the 1980 – 1986 eruption of Mount St. Helens, advances in our understanding of morphological evolution and kinetics of lava domes (crystal growth and nucleation) were made (e.g. Cashman, 1988; Geschwind et al., 1995). Moreover, the breadth of eruptive styles and improvements in monitoring techniques helped to improve and refine models of lava dome growth (Calder et al., 2015).

The ascent of magma in volcanoes is typically accompanied by numerous earthquakes, the release of magmatic gases, and surface deformation. A systematic volcano monitoring network to detect these phenomena is therefore needed. During the last years, detection systems and techniques have improved, reaching a high level of sophistication. In addition, the creation of advanced models for volcanic processes is improving the interpretation of monitoring data. Some of the techniques commonly used are: seismic monitoring, deformation monitoring (interferometric synthetic aperture radar InSAR and/or GPS), gas emissions monitoring (DOAS, ultraviolet cameras), and observations through regular cameras. All these techniques can be combined to give a much more complete and informative picture of a volcano's behavior. Other monitoring techniques include magnetometry (Fougere et al., 1980; Nakamura et al., 1912), gravimetry (Battaglia et al., 2008), portable ground radar (Gómez-Ortiz et al., 2006) and infrasound (Fee and Matoza, 2013). The last two are already being deployed to document explosive eruptions and ash clouds. Muon tomography, a non-invasive technique that uses cosmic ray muons to image internal structures, can also be used (Gómez, 2019). It holds promise for imaging the subsurface of lavas, but this method will need further development to become widely used (Sparks et al., 2012). Finally, thermal imaging is employed to detect surface manifestations

of volcanic unrest, such as increased fumarole or vent temperatures due to magma ascent from depth (Carn, 2015).

Taking into account all the monitoring techniques aforementioned, it is obvious that one of the required and useful techniques to study lava domes is imaging. Because surface deformation is important during lava dome growth, aerial photographs are a good record to look at these changes and compare them through time. In addition, changes in surface temperature, and other thermal features should be monitored with thermal surveillance.

Volcanoes can generate a wide variety of events that represent risks for the environment, living beings and infrastructures. Effusive eruptions of lava domes can be dangerous, exposing populations to prolonged periods of hazards ranging from ash falls to violent dome collapse events. Hazards associated to these lava dome collapses include pyroclastic flows and surges, and sometimes lateral blasts, lahars, and debris avalanches (e.g. Belousov et al., 2007; Calder et al., 2015; Komorowski et al., 2013; Maeno et al., 2019; Ogburn et al., 2015; Reyes-Dávila et al., 2016). Lava domes associated to explosive eruptions can produce ash falls, ballistic showers, and sometimes, eruptive column collapse and pyroclastic flows. Other hazards are strongly linked to external forces such as rainfall and/or regional earthquakes (Calder et al., 2015). In tropical regions, seasonal episodes of heavy rain can lead to lahars if loose material is readily available, and dome complexes made of old and hydrothermally altered lavas are prone to sector collapses forming debris avalanches (e.g. Sparks et al., 2002). The complexity of lava dome eruptions from dynamics of magma ascent in conduits to extrusion, emplacement, and associated-related hazards, make the study of lava domes challenging, requiring an integrated multidisciplinary effort from monitoring to hazard mitigation (Calder et al., 2015).

In this work, a thermal and morphological analysis of a lava dome at Volcán de Colima will be done for the period 2013 to 2016. We will use aerial photographs taken during flights around the volcano to describe and define important phases during the process of growth, as well as identify the principal features of the dome such as shear lobes, spines, talus, carapace, blocks, explosion pits, and compressional ridges. This analysis will help to have a better understanding about the eruptive dynamics occurring during the different growth phases of the lava dome. Additionally, thermal images taken during the same flights with a thermal camera will be used to detect changes in volcanic heat distribution, fumarole fields and other details of the lava dome surface such as hot vents, incandescent cracks, etc.

Finally, a combination of digital photographs and thermal images will be used to calculate effusion rates of the 2016 lava dome. It will provide important information of the relationships between effusion rate and dimensional or morphological characteristics, such as flow length and area, types of lava transitions, and tube formation and size (Harris et al., 2007). A further motivation to develop this study is to contribute to the understanding of the processes behind the growth and destruction of a lava dome in one of the most active volcanoes in Mexico.

1.1. Statement of the Problem

Lava domes are important components of the long-term activity of many volcanoes, and major explosive activity occurs in association with dome growth, causing the most significant and deadly eruptions such as Unzen, 1993 (Gomez, 2006) and Merapi, 2010 (Surono et al., 2012). In addition, lava dome behavior includes surprising shifts between effusive and explosive activity, fast changes in lava composition, and changes in the growth process (exogenous or endogenous) during their formation. To better mitigate the hazards caused by lava domes, it is fundamental to understand the processes that govern their stability, and unpredicted behavior. In this case, Volcán de Colima is one of the most hazardous volcanoes in Mexico, with an important effusive activity associated with growth of lava domes in the summit crater. It is therefore important to study the processes involved in dome growth, and the causes that lead to their destruction.

1.2. Objectives

Understanding the causes, effects and possible patterns of dome formation will help to apply a better assessment of risk and hazard in the two states around the volcano, Colima and Jalisco. Therefore, there are three main objectives for this project:

- To describe physical and morphological changes during the growth phases (2013-2016) of the lava dome in Volcán de Colima using high resolution photographs taken on monitoring flights. The aim is to detect changes in surface deformation, features which precede or come after the formation of the dome, and textural changes of the material.
- To study the thermal evolution of the growing lava dome, and to extract quantifiable temperature data from thermal surveys in order to understand processes that govern the overall development and stability of the lava dome (Hutchison, 2011).

- To calculate effusion rates for the 2016 lava dome, using dimensions of the crater and lava dome at the beginning, during, and at the end of its formation.

2. Volcán de Colima

Volcán de Colima is one of the most active volcanoes in North America (Navarro-Ochoa et al, 2002), belonging to the western sector of the Trans-Mexican Volcanic Belt (TMVB) (Hutchison, 2011). The volcano is located on the border between the states of Colima and Jalisco, 485 km west of México City (Fig. 2.1). Its coordinates are 19°30' N and 103°37' W. It is part of a chain of three composite volcanoes located at the center of a large N-S oriented graben known as the Colima Volcanic Complex (CVC) (Fig. 2.2).

Fig. 2.1. *Location of Volcán de Colima. (A) Location map of México showing the Colima state. Retrieved from pickatrail.com (B) Aerial picture of Volcán de Colima, located on the border between Colima and Jalisco states (Google Maps, 2019). (C) Aerial SE-NW view of the Volcán de Colima summit 2019.*

2.1. Geological Background

According to Ferrari et al. (2011), the Trans-Mexican Volcanic Belt is the largest Neogene volcanic arc in North America, which comprises an area of approximately 160,000 km^2 and a length of almost 1000 km in central Mexico (Fig. 2.2). The Quaternary volcanism of the

8

western part of the TMVB is the result of two tectonic processes that affect the region: (1) the subduction of the Rivera plate beneath the North American plate (Fig. 2.2), and (2) the development of the rift triple junction (Fig. 2.3) (Cortés et al., 2010).
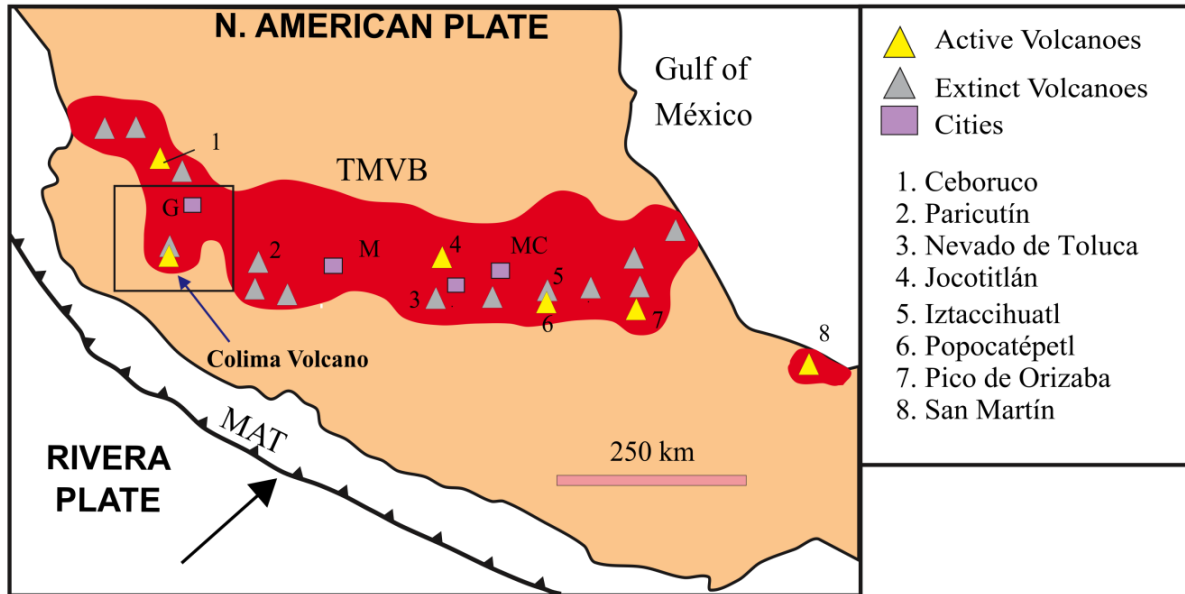

Fig. 2.2. *Location of Volcán de Colima in the western part of the Trans-Mexican Volcanic Belt (TMVB). MC: Mexico City, M: Morelia, MAT: Middle American Trench. Taken from Saucedo et al. (2005).*

The triple junction located in the western sector of the TMVB is the intersection of three long fault systems, with orientations approximately N-S, E-W and NW-SE (Campos-Enríquez and Alatorre-Zamora, 1998). The fault system defines three elongated depressions called the Colima, Chapala, and Tepic-Zacoalco grabens which are separated by angles approximately 100º, 115º and 145º, counterclockwise from the Colima Graben (Fig. 2.3) (Cortés et al., 2010; Luhr et al., 1985). The northern Part of the Colima Rift is delineated by NNE-SSW oriented faults. In the southern part of the CVC, the Colima rift cuts the limestone platform of the Colima Basin (Cortés et al., 2010). According to Garduño-Monroy et al. (1998), the northern and southern parts of the Colima Rift seem to be separated by the CVC. However, the trace of a structure that could be controlling the geometry of the Colima Rift and the volcanic activity of the CVC has been observed on both NE and SW sides of the CVC. This structure was denominated the Tamazula Fault (Fig. 2.4). It is a basement structure with NE-SW direction and a length greater than 160

km. Tamazula fault has governed the geometry of the Colima rift, and the volcanic evolution of the CVC (Garduño Monroy et al., 1998).
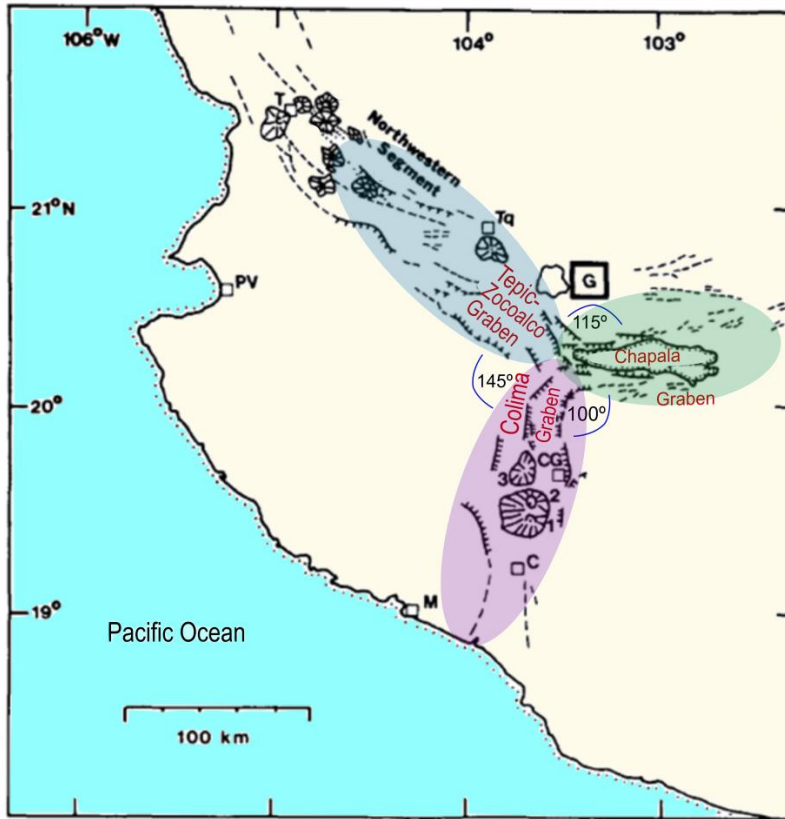

Fig. 2.3. *Map of the western part of the TMVB that shows the graben triple junction, and Colima volcanic complex. 1: Volcán de Colima; 2: Nevado de Colima; 3: Volcán Cántaro; T: Tepic; PV: Puerto Vallarta; Tq: Tequila; G: Guadalajara; CG: Ciudad Guzmán; C: Colima; M: Manzanillo. Edited from Luhr et al. (1985).*

Fig. 2.4. *Digital elevation model of the Colima volcanic complex that shows steeper slopes in dark-red and gentler slopes in pale gray. The image displays the NE-SW trace of the Tamazula fault and the Alceseca-Atenquique graben across the southern portion of the Colima volcanic complex. EC: EL Cántaro; NC: Nevado de Colima; PF: Paleofuego; CV: Colima Volcano. White asterisks indicate ^{14}C dates in years before present (BP). Edited from Cortés et al. (2010).*
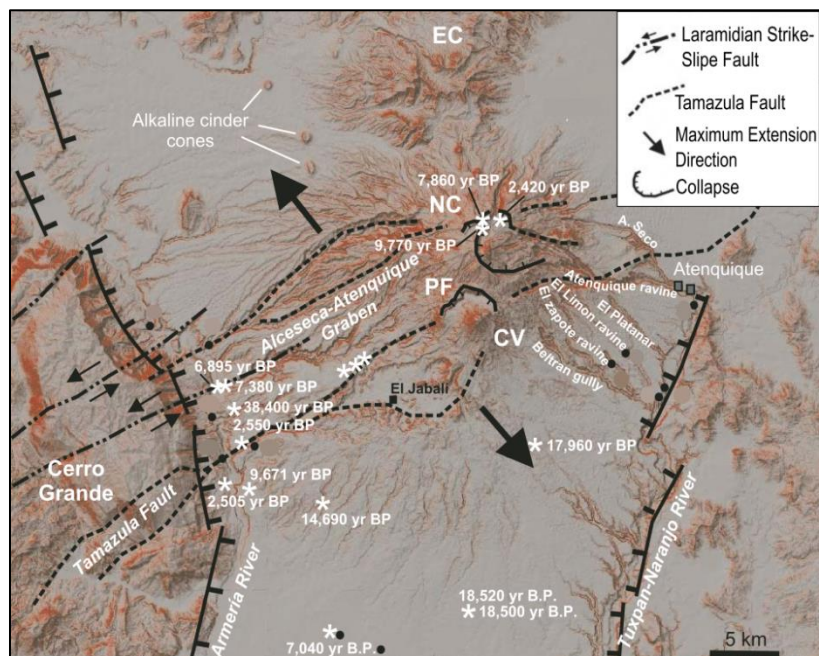
The Colima Rift is filled by a ∼1 km-thick sequence of quaternary lacustrine sediments, alluvium, and colluvium, covering the ~3000 m-thick volcanic pile from the CVC (Fig. 2.5) (Norini et al., 2010). Based on Luhr & Carmichael (1980) the Quaternary Colima Volcanic Complex is roughly circular with a radius of approximately 12 km. During the past 1 My, calc-alkaline volcanic activity has been primarily confined to the southern graben floor, building a north-south oriented chain of three andesitic composite volcanoes. From the youngest to the oldest, these are: Volcán Cántaro (~ 1-1.7 Ma; 2900 masl), Nevado de Colima (~ 0.53 Ma; 4255 masl), and Volcán de Colima or Volcán de Fuego (in the last ~50 ka; 3860 masl) (Cortés et al., 2010; Luhr et al., 1985; Norini et al., 2010).
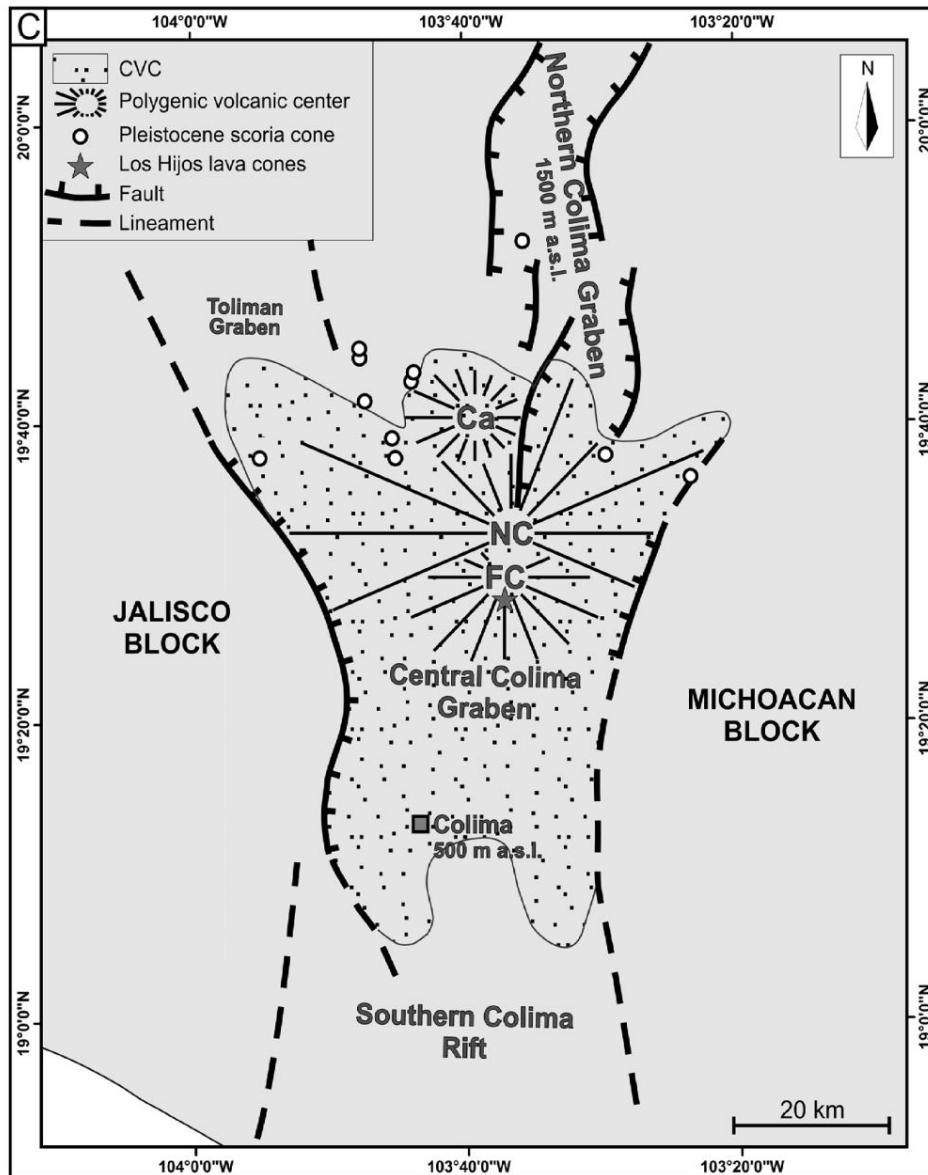
Fig. 2.5. *Schematic map of the Colima Rift and the Colima Volcanic Complex. Ca: Volcán Cántaro; NC: Nevado de Colima; FC: Fuego de Colima. Edited from Norini et al. (2010).*

Volcán de Colima (Fig. 2.6) is the most active volcano in México. The current edifice is a stratovolcano displaying interbedded lava flows and pyroclastic layers that occupies an area of 20 km^2 with a total volume of ~9-10 km^3. Pyroclastic flows have traveled up to 15 km downslope, while lava flows reached up to 5 km from the summit (Cortés et al., 2010). The dominant eruptive product of Volcán de Colima is hornblende-andesite.
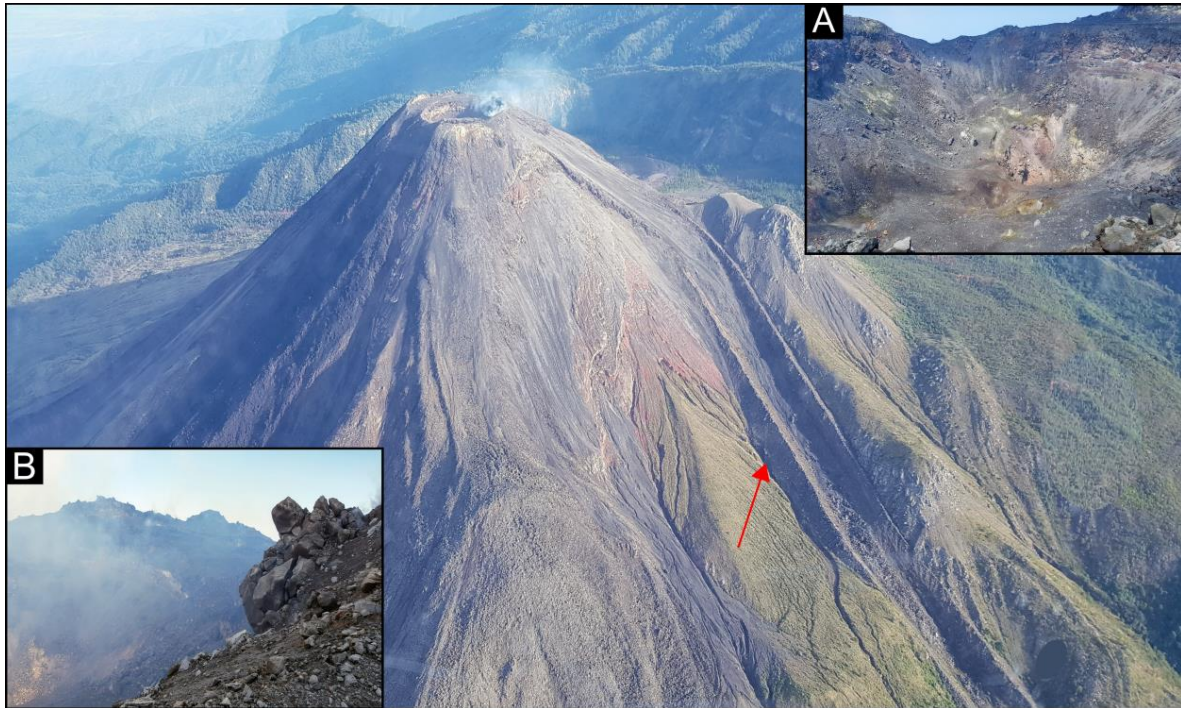
Fig. 2.6. *Aerial photograph of the south-eastern flank of Volcán de Colima in August 2019, showing the 1975-76 lava flow (red arrow) as well as aprons of recent pyroclastic deposits. A) Zoom-in of the crater. B) Gas emissions in the crater. Pictures: Andrea Tonato.*

The historical eruptive activity has been characterized by a complex succession of effusive lava dome or lava flow eruptions with associated block and ash flows, and explosive eruptions of varying magnitude that have produced numerous and diverse types of pyroclastic density currents (PDCs) (Navarro-Ochoa et al., 2002). At least 29 significant eruptions have been recorded during the last 400 years (Luhr and Carmichael, 1980). As a result of this activity, the volcano is covered by a thick mantle of hornblende-bearing pyroclastic deposits (Luhr and Carmichael, 1980), while the summit consists of unsorted lava blocks (Taran et al., 2002).

Based on all the registered eruptions, this volcano tends to have three types of eruptions: Pelean, that results from gravitational collapse of domes; Vulcanian, which is an explosive eruption due to a plug of the conduit by the lava dome; and Plinian, that is a sustained Vulcanian eruption (Alle, 1983; Navarro-Ochoa et al., 2002; Saucedo et al., 2005). Additionally, the activity of Volcán de Colima has shown a ~100 year cycle, characterized by lava flow effusion, dome growth and moderate explosions (Zorn et al., 2019). The last large eruptions occurred in 1818 and 1913 which were the first well documented Plinian eruptions (Macías et al., 2017). The 1818 eruption destroyed a lava dome, and its slag and

ash reached the cities of Guadalajara, Zacatecas, Guanajuato, San Luis Potosí and México City (Macías et al., 2006). The 1913 eruption removed about 100 m of the existing edifice and left a summit crater that was 450 m in diameter and at least 350 m deep (Waitz, 1935). In 1931, the presence of a large active lava dome inside the 1913 crater was discovered, and quasi-continuous extrusion was observed over the following 29 years, sometimes resulting in overflowing over the crater rim (Navarro-Ochoa et al., 2002).

Other effusive eruptions occurred in 1975-1976 (Fig. 2.6) and 1981-1982, both preceded by emplacement of block and ash flows (Navarro-Ochoa et al., 2002). Events occurred in 2004-2005 that were characterized by several episodes of dome growth and collapse, accompanied by the emplacement of pyroclastic density currents that reached up to 7 km from the volcano's summit (Capra et al., 2016). Activity in recent years comprised lava dome growth and destruction, which will be detailed in the next section.

2.2. Lava Dome Growth

A study of lava dome growth at Volcán de Colima from 2007 to 2011 was performed by Hutchison (2011). It involved the use of a high spatial resolution infrared dataset collected during airborne surveillance to investigate the thermal evolution of the growing lava dome. As a result, Hutchison (2011) proposed a three stage eruption chronology on the basis of notable changes in growth patterns, styles and morphologies. Stages I and III were defined by exogenous growth, while Stage II involved endogenous growth. In addition, thermal image analysis provided clear precursors to the formation of thermal features around the lava dome, and to the eruptive stages.

Moreover, physical and thermal observations were linked to heat models, to explain the governing physics during lava dome growth. An 18 month-long period of volcanic and seismic quiescence started in June 2011 (Fig. 2.7), following this 2007-2011 episode of dome growth (Zobin et al., 2015).
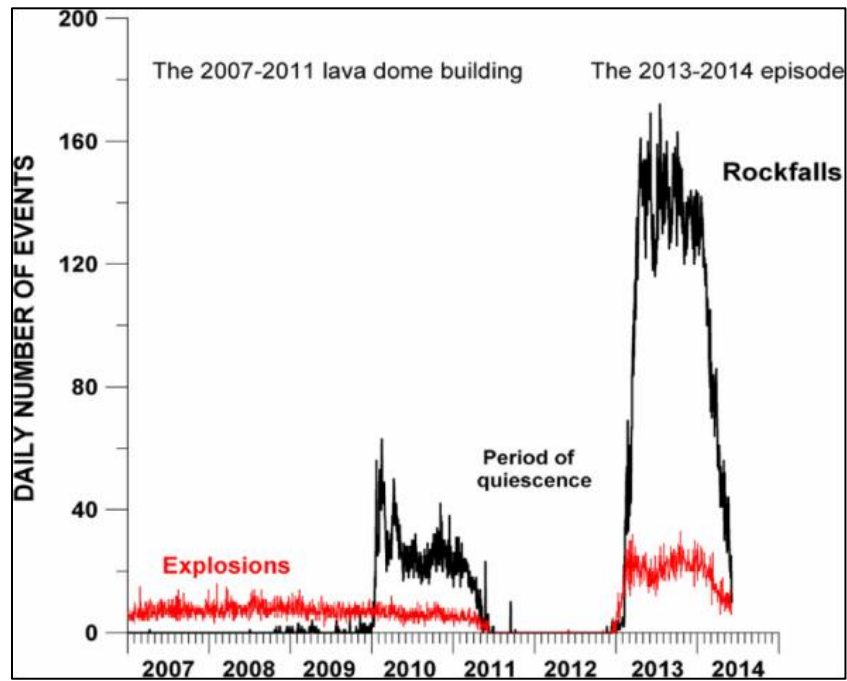
Fig. 2.7. *Seismic activity at Volcán de Colima associated with the 2007-2011 lava dome building and the 2013-2014 eruption episode. Taken from Zobin et al. (2015).*

The activity picked up from 6th to 29th January 2013, with vulcanian explosions resulting in the formation of a new crater within the 2007-2011 lava dome (Arámbula-Mendoza et al., 2018; Reyes-Dávila et al., 2016; Zobin et al., 2015). From February to October 2013, the new lava dome was built, and from October onwards, effusive activity accompanied by minor explosive events occurred (Reyes-Dávila et al., 2016; Zobin et al., 2015). At the end of November 2013, the building of the lava dome was practically finished, and the activity of the volcano decreased until June 2014 (Zobin et al., 2015). In September 2014, Reyes-Dávila et al. (2016) reported increased activity at the volcano. On 3rd of January 2015, explosive activity occurred, generating a 2 km-long block and ash flow to the N flank causing the gradual destruction of the dome. A new dome was emplaced in May 2015 (Reyes-Dávila et al., 2016).

Finally, without strong precursors, on the 10th and 11th of July 2015, the dome collapsed during an explosive eruption, forming a PDC of 9.1 km in length (Fig. 2.8) (Capra et al., 2016; Zobin et al., 2015). Moderate activity, including vulcanian explosions, dome growth and lava flow effusion, continued until February 2017, when the most recent active period terminated (Zorn et al., 2019).
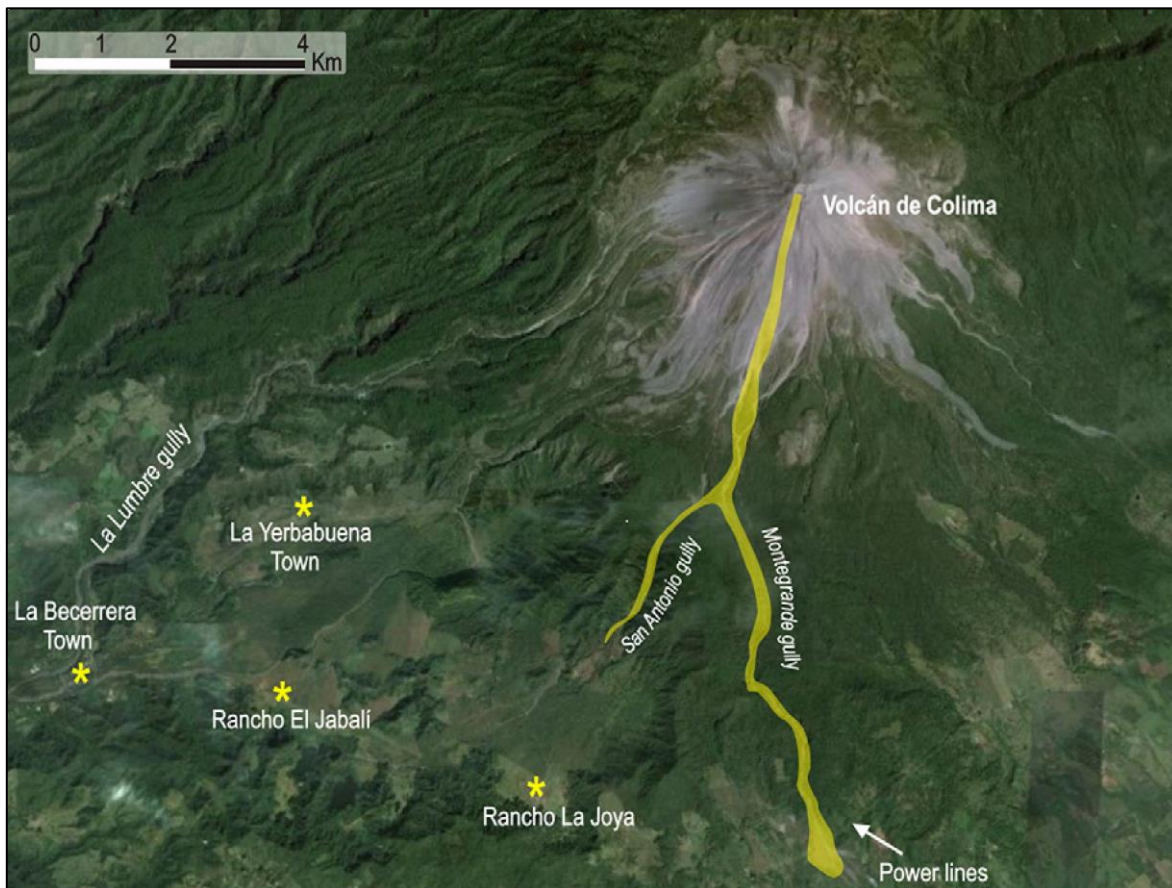
Fig. 2.8. *Satellite image of Volcán de Colima showing the distribution of the July 2015 PDCs along the Montegrande and San Antonio ravines. The yellow stars show the locations of nearby communities and towns. Edited from Reyes-Dávila et al. (2016).*

2.3. Effusion Rate

The effusion rate is the rate at which lava is erupted, or in this case, the rate at which a lava dome is emplaced within the crater (Harris et al., 2007). This rate controls the way in which a lava body grows, extends and expands, influencing its length, width, thickness, volume and/or area, no matter whether the growth process is exogenous or endogenous (e.g. Baloga and Pieri, 1986; Harris et al., 2007; Murray and Stevens, 2000). Estimating the effusion rate is one of the primary objectives of monitoring effusive volcanic activity. Changes in the rate can be used to determine whether activity is increasing or decreasing, or to assess the long-term behavior and hazard associated with the system (Calvari et al., 2010; Harris et al., 2007, 2000).

3. Methodology

The data used for this project was provided by Centro de Investigación e Intercambio en Vulcanología (CIIV) which belongs to the Faculty of Science in the University of Colima in México. CIIV has been running since 2004, with a main aim of increasing knowledge of Volcán de Colima and other volcanoes in México.

3.1. Monitoring flights

Over-flights take place at Volcán de Colima once every 1-2 months. It has been an important monitoring technique for CIIV since February 2007, the time of dome growth onset. In order to obtain good data during the flight, the weather should be clear with no clouds on the summit, and it has to be early in the morning (7-8 am local time) in order to optimize sunlight and minimize solar heating of the edifice which could obscure the volcanic thermal signature (Hutchison, 2011).
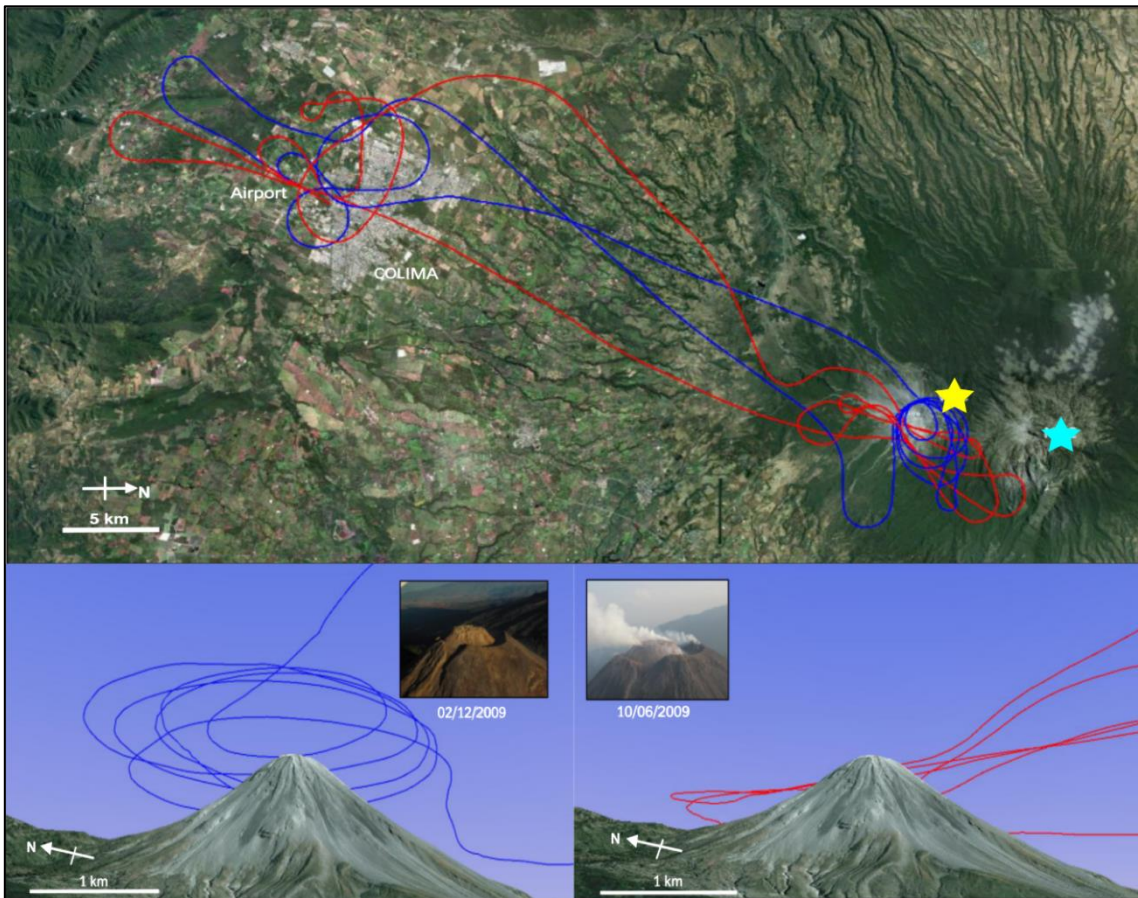
Fig. 3.1. *Map showing flight trajectories on June and December 2009. Flight trajectories depend on the summit conditions. The blue line shows a typical flight where there is a clear summit. The red line shows the path that must be taken when a degassing or explosive event is occurring. The yellow star marks Volcán de Colima, and the turquois star marks Nevado de Colima. Lower images show a 3D perspective of the flight paths at the exact altitude. Digital photographs show the condition at the summit on the day of flight. Edited from Hutchison (2011).*

Flights last 20 to 30 minutes, and cover in circles the entire edifice, giving complete spatial coverage of the summit (Fig. 3.1). When there is high volcanic activity during the flight such as degassing or explosive events, the trajectory must be altered due to dispersed ash or gas plumes. There are three main datasets that are collected during the flight:

- Photographs using digital cameras (always)
- Infrared images from a hand-held thermal camera (always)
- GPS tracks of the flight path (infrequently)

18

3.2. Digital Photographs

Aerial photography is the most basic and cheapest method for volcano monitoring. It is used during volcanic unrest to quantify areas of surface deformation, and at erupting volcanoes to quantify the volume of erupted material such as lava flows, volcanic domes and pyroclastic density currents. At Volcán de Colima, photographs are taken as many as possible around the volcano. It is important to record every structure such as lava flows, lava domes, vent areas, and other eruptive products in order to get a better vision of the morphological changes through time. In addition, concentration and a steady hand are some of the traits that permit good data collection.

For this project, blurred photographs were not considered, nor those where the summit or lava dome were not visible. At the end, we analyzed approximately 2400 good digital photographs. The typical time spacing for a set of good photographs (~66) is a month, having the largest time gap of 3 months.

3.3. Thermal Monitoring

Thermal cameras have been introduced in volcanology to analyze a number of volcanic processes. According to Calvari et al. (2004), this method allows the detection of changes in heat distribution on volcanic surfaces which can be used to:

- Recognize magma movements within the summit conduits, and detect the upward movement of shallow fractures in the ground filled by hot magma
- Distinguish active lava flows and lava tubes
- Analyze the evolution of fumarole fields and eruption plumes
- Obtain effusion rates for active lava flows
- Recognize storage of magma at shallow depth
- Reveal failure planes and instability on the flanks, and the opening of fissure systems just before flank collapse at active volcanoes

The thermal dataset of Colima provides high spatial resolution images offering a complete coverage of the summit crater and domes whenever present. It permits a study of the long-term (3 years) evolution of the lava dome. In this case, a Jenoptic VarioCAMHR was used to collect the datasets (Fig. 3.2). This camera has a wavelength range of 8-14 μm, lens of 75

mm, field view of 12×9 ° and 640×480 pixels (Hutchison, 2011). According to Hutchison (2011), six sources of error which can affect the raw temperature data are identified:

1. Instrumental uncertainties such as: noise in the equipment and poor focus. Jenoptic reports ±1.5 ℃ accuracy for targets at 0 – 100 ℃, and ±4 – 8 ℃ for volcanic features at 200 – 400 ℃. Correction: there are no corrections; however, these uncertainties are typically small relative to the magnitude of the measurements. It is possible to activate the auto-focused tool so that poorly focused images are discarded prior to processing.

2. Atmospheric transmissivity: attributed to weather conditions and path length which attenuate the original signal. Correction: we assume path-length is 100 m and that relative humidity and ambient temperature are constant along this path.

3. Solar radiance which contributes to heating the dome surface. Correction: monitoring flights must take place early in the morning between 7 to 8 am local time.

4. Variable path length: pixels covering the ground are not constant because measurements are taken at different distances representing an error of ±40 ℃ (Hutchison et al., 2013). Correction: GPS data are not available for each flight; therefore, it is not possible to correct maximum temperatures for each image individually. This represents the largest uncertainty in maximum temperatures.

5. Emissivity constant which changes with the viewing angle. Correction: we assume that a default camera value of 0.95 is relevant, and constant.

6. Volcanic ash and gas can also attenuate the signal. Correction: No correction in the camera.
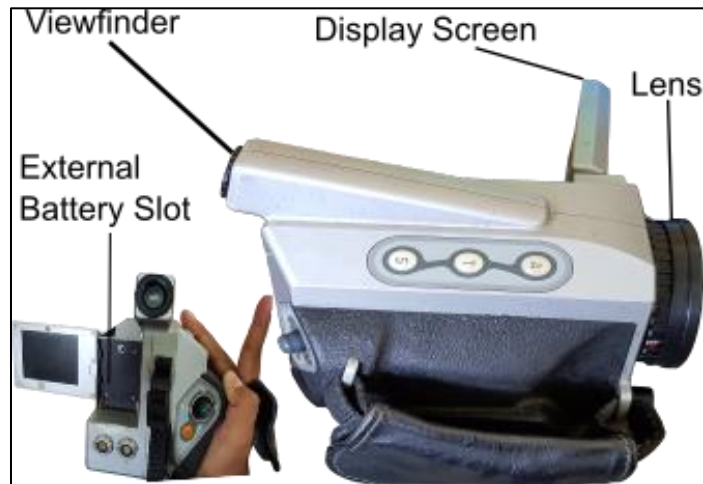
Fig. 3.2. *Handheld Jenoptic Thermal camera used in this study. The figure shows the camera that operated during monitoring flights at Volcán de Colima (2013-to present). Pictures: Andrea Tonato.*

Collected images are uploaded to the IRBIS 3 Professional® software and assessed for quality. In order to use images in the analysis, they must fulfill the following criteria:

- Images must be well focused. Images where the camera is out of focus or where volcanic processes distort the image must be rejected.
- For this study, the image must have a complete coverage of the entire dome.
- Images must contain only the volcanic edifice, the ones which show plane wing must be deleted.

To use the data as a monitoring tool, regions of interest (ROI) were picked. ROI can be lava dome top, lava dome sides, lava dome lobes, the whole dome, fumaroles and volcano flanks (Hutchison, 2011), from which the temperatures are extracted.

3.4. Effusion Rate Calculations

For the effusion rate calculation, we chose to analyze the lava dome growth in 2016 only, because of the clearness of the growth process in digital photographs. It allows a more accurate measurement of distances between points of reference in order to calculate volumes. The principal features taken as reference points were the crater diameter (~300 m) and depth (~60 m), and lava dome width (~25 m) and height (~10 m) from February 2016 (Varley, 2016) (Fig. 3.3).
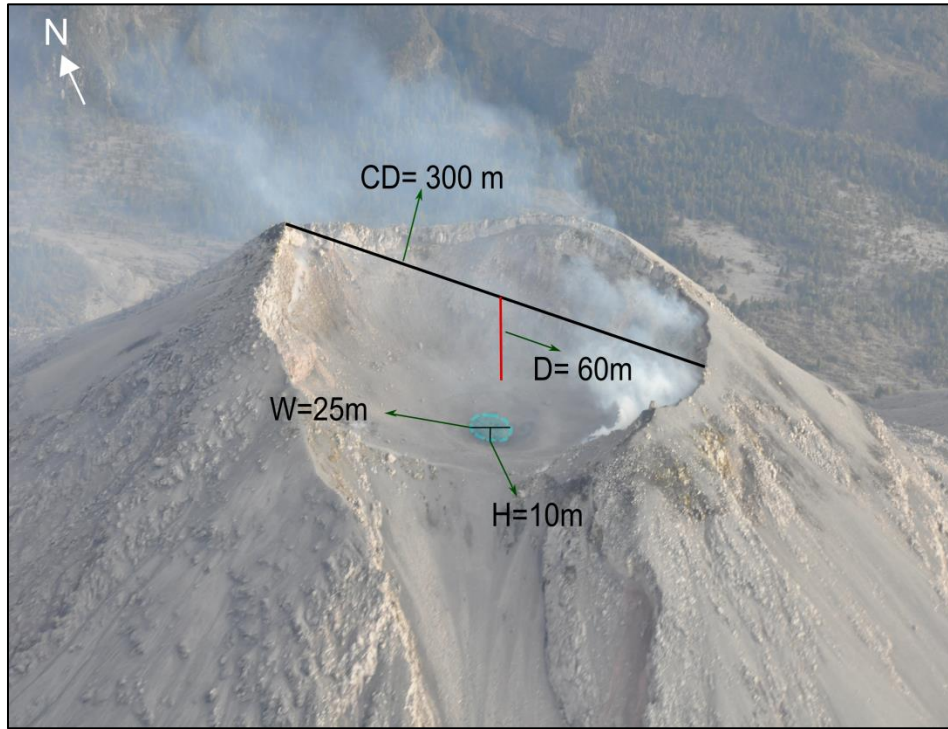
Fig. 3.3. *Measurements of reference used to estimate the volume of the growing lava dome in 2016 for effusion rate calculations. The figure shows the estimated dimensions taken during a monitoring flight (Varley, 2016). CD: crater diameter; D: depth; W: lava dome width; H: lava dome height.*

In order to calculate the volume of the dome, we defined two main geometries due to the changes in morphology during growth. From February to April 2016, we assumed that the shape of the lava dome was a half-sphere, thus the formula used to calculate the volume was:

$$V_d = \frac{2\pi r^3}{3}$$

Eq. 3.1

Where V_d represents the lava dome volume, and r is the radius of the lava dome. On the other hand, for the period between May and the end of 2016, the best representation of the lava dome shape is a frustum (Fig. 3.4), thus the formula used to calculate the volume was:

$$V_d = \frac{1}{3}\pi h(r^2 + rR + R^2)$$

Eq. 3.2

Where h is the height of the lava dome, r is the shortest radius of the lava dome, and R is the longest one.
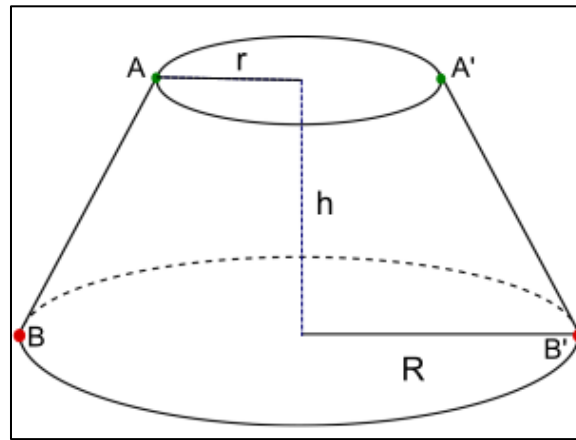
Fig. 3.4. *Frustum of a circular cone. The figure shows the structure of a frustum and the required lengths needed in order to calculate its volume. AA'/2 = r; BB'/2 = R; H: height of the lava dome. Edited from: Simmons (2017).*

Using the difference in dome volume and the time during which these changes occurred, it is possible to obtain the effusion rate. However, the obtained values represent the bulk volume without considering vesicularity of the neither lava nor void space between the blocks of the dome. To correct for this we convert from measured volume to dense rock equivalent (DRE). In this work, conversion to DRE volumes was made using a multiplicative correction of 0.844 which was calculated by Sparks et al. (1998) assuming that andesitic lava has a density of 2600 kg/m^3, an average vesicularity of 13% and 3% void space (e.g. Hutchison, 2011; Ryan et al., 2010). However, the bulk vesicularity and pore space in the dome (including talus) vary through time and cannot be measured continuously (Ryan et al., 2010; Sparks et al., 1998). According to Sparks et al. (1998), the photographic method to estimate volume of the lava dome are better than 15% accurate. Indeed, their photographs were taken from fixed GPS positions, so they could observe topographic features of known height which was useful to established scales between photographs using trigonometry and triangulation. In this thesis, uncertainty was higher due to the little information about the first estimate of the crater size, and the random direction and distance of the position where the pictures were taken. Additionally, considering the unknown position and angle of the diameter and depth measured by Varley (2016), and the error caused by the multiple measurements in the photographs, we assumed an uncertainty of 20 % for our calculations of volume and effusion rates.

4. Results

4.1. Morphological Changes

Digital photographs showed important changes in short periods of time. In February 2013, a new lava dome started to grow rapidly within the crater. By June 2013, the lava dome reached its maximum height, completely filling the old lava dome crater (Fig. 4.1).

Fig. 4.1. *Morphological changes of the lava dome during 2013. The figure shows the flanks of the volcano that have been taken as a reference of change due to their sharp morphologies. Black empty spaces are due to the lack of clear and/or high-resolution photographs.*

From June onwards, the collapse of the new lava dome started. Degassing during 2013 is relatively low, and it is possible to see that the common zones for fumaroles are the crater rim and the summit of the new lava dome. During 2014, there was a continuous extrusion of material that fell on the flanks during the collapse of the new lava dome. Since July 2014, degassing increases, so that at the end of the year observations of the crater are difficult. Between August and October, new material with different blocky-surface texture was extruded (Fig. 4.2).

Fig. 4.2. *Morphological changes of the lava dome during 2014. The pictures clearly show high degassing starting in July.*

In 2015, there is continuous degassing in the summit, but the most representative changes occur in the morphology of the whole volcano summit. By February, the new lava dome is completely gone, leaving a small portion of the old dome edifice with a concave shape crater. In June, the crater is filled again by extruded blocky material which is evacuated

very rapidly. This creates an almost empty crater by August where the whole old dome has completely disappeared, leaving the volcano summit with a concave shape (Fig. 4.3).

Fig. 4.3. *Morphological changes of the dome and summit during 2015.*

The most important event during 2016 is the growth of a new lava dome starting in February (Fig. 4.4). This lava dome grew slowly until April, after which the extrusion rate

increased, completely filling the crater by July. Some of this material is evacuated during the following months, with a less-filled crater in September.
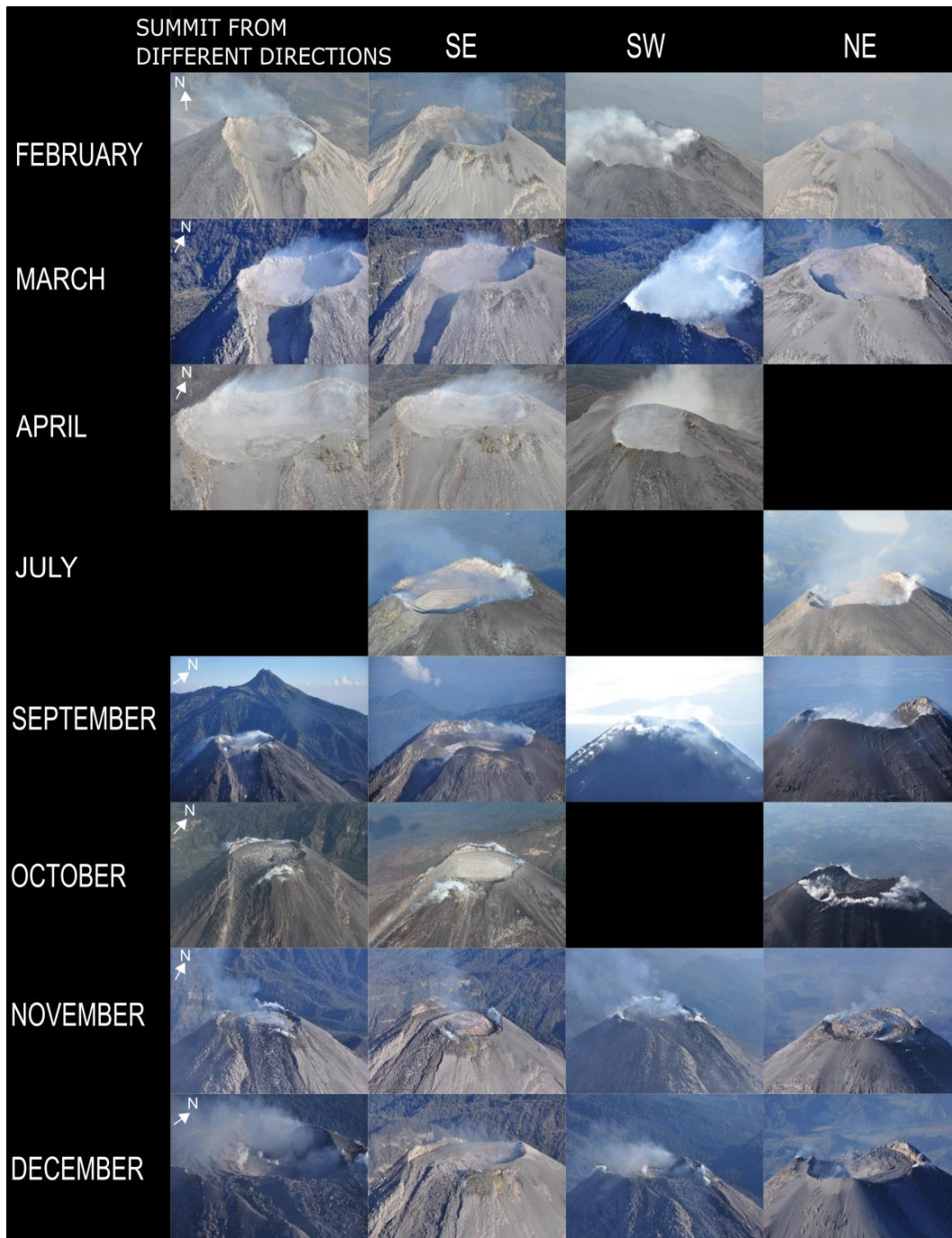
Fig. 4.4. *Morphological changes of the volcano summit during 2016. The figure shows that since February, a new lava dome starts growing.*

Growth started again in October and persisted until November, with material falling down the flanks. A crater-like shape is observed at the center of the lava dome in December,

contrasting with the convex shape of the rest of the dome. We can observe a low continuous degassing throughout the year.

To summarize, we observed changes in the Colima crater morphology during the period 2013-2016, which are related to different phases of lava dome formation such as growth, collapse and destruction. We also detected changes in the degassing regime, with the most abundant degassing occurring in 2014-2015. The changes in the texture of the extruded material at the summit will be detailed in the next section. It is noteworthy that all these processes are complex and occur in very short periods of time.

4.2. Changes in lava texture

The different and complex processes of growth, collapse and destruction at Volcán de Colima manifest through changes in the texture of the extruded lavas (Fig. 4.5). During the whole period 2013-2016, we define four different textures of lava:

- **Type I**

It is characterized by a fractured lava surface, and grey-angular blocks which varies their size in different phases. This lava represented the most viscous material extruded during 2013-2016 (Fig. 4.5A, C and E). It principally occurred during the growth of lava domes, and their collapsing phases (February 2013-August 2014, June 2015, February-April 2016, and November 2016).

- **Type II**

It is characterized by fragments of spongy lava surface and black-angular clinker fragments (uniform in size) which are smaller than the previous type. This indicates a decrease in viscosity of the magma, and increase in temperature (Fig. 4.5B). This type of material was observed during periods of high explosive activity (September 2014-January 2015).

- **Type III**

It is characterized by a rough lava surface similar to a fresh concrete mixture. No blocks are visible; the extruded material is grey with shallow curvilinear fractures and seems to be fine material (Fig. 4.5D). This occurred during July-October 2016, when new material was filling the crater.
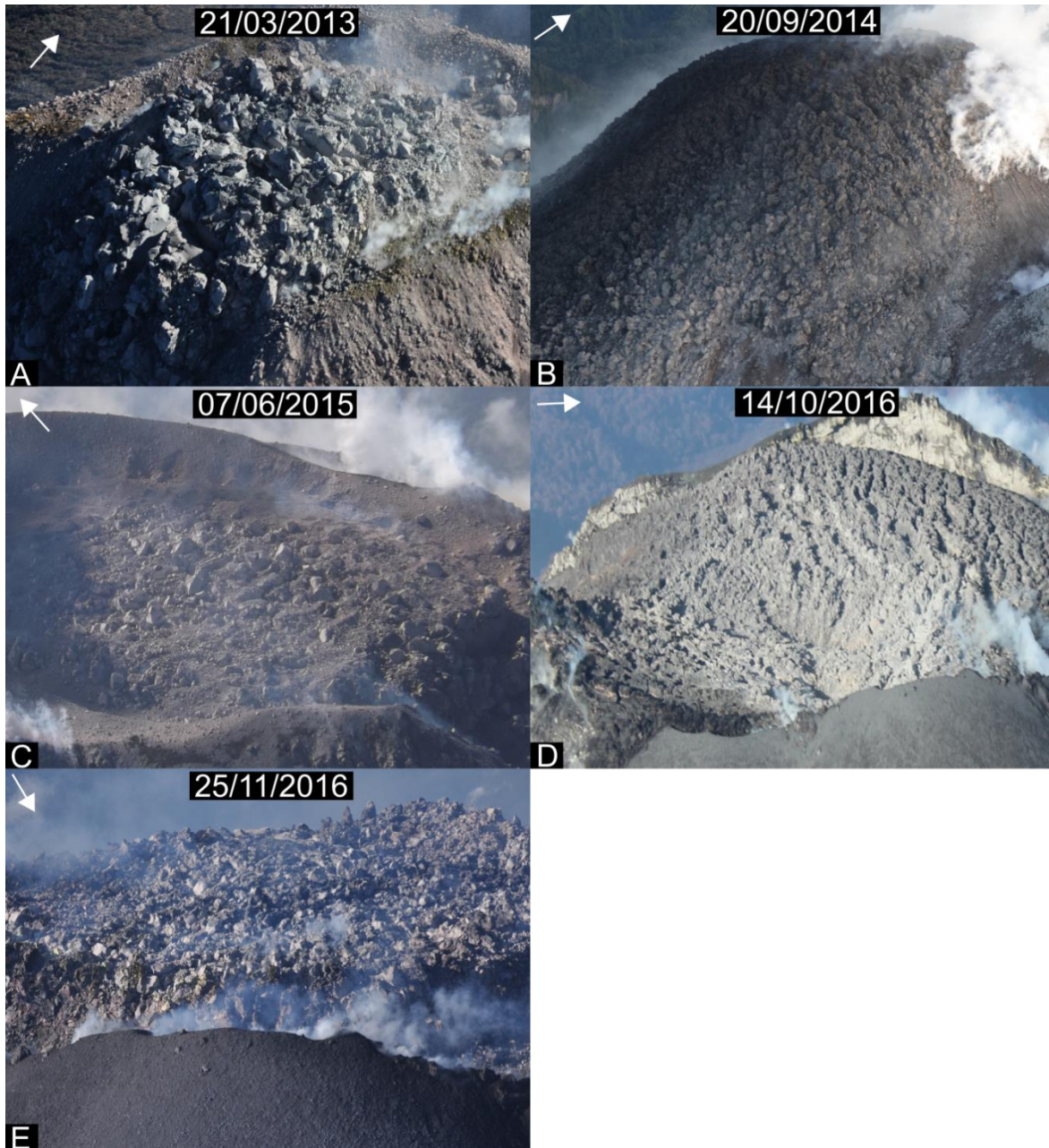
Fig. 4.5. *Digital photographs of the period 2013-2016 at Volcán de Colima summit. The figures show the differences in texture of the extruded material of Volcán de Colima. North is represented by the white arrow. A) Representative picture of texture type I; B) Representative picture of texture type II; C) Representative picture of texture type I, and finer material; D) Representative picture of texture type III; E) Representative picture of texture type I, and smaller blocky material.*

4.3. Thermal Changes

Thermal images were taken during monitoring flights to observe changes in temperature with time at Volcán de Colima. During the whole period 2013 - 2016, the maximum observed temperatures vary from 150 ℃ to 500 ℃. Three images were chosen as

30

representative of the growing new lava dome during the period of observation in 2013 (Fig. 4.6 - Fig. 4.8).

In January 2013, we can see that the maximum temperature is 201 ºC, and it is located on the S top flank of the old lava dome (Fig. 4.6). In general, the hottest parts are located at the S upper part of the old lava dome. Other hot locations are around the crater and lava dome rims where fumaroles can be seen.
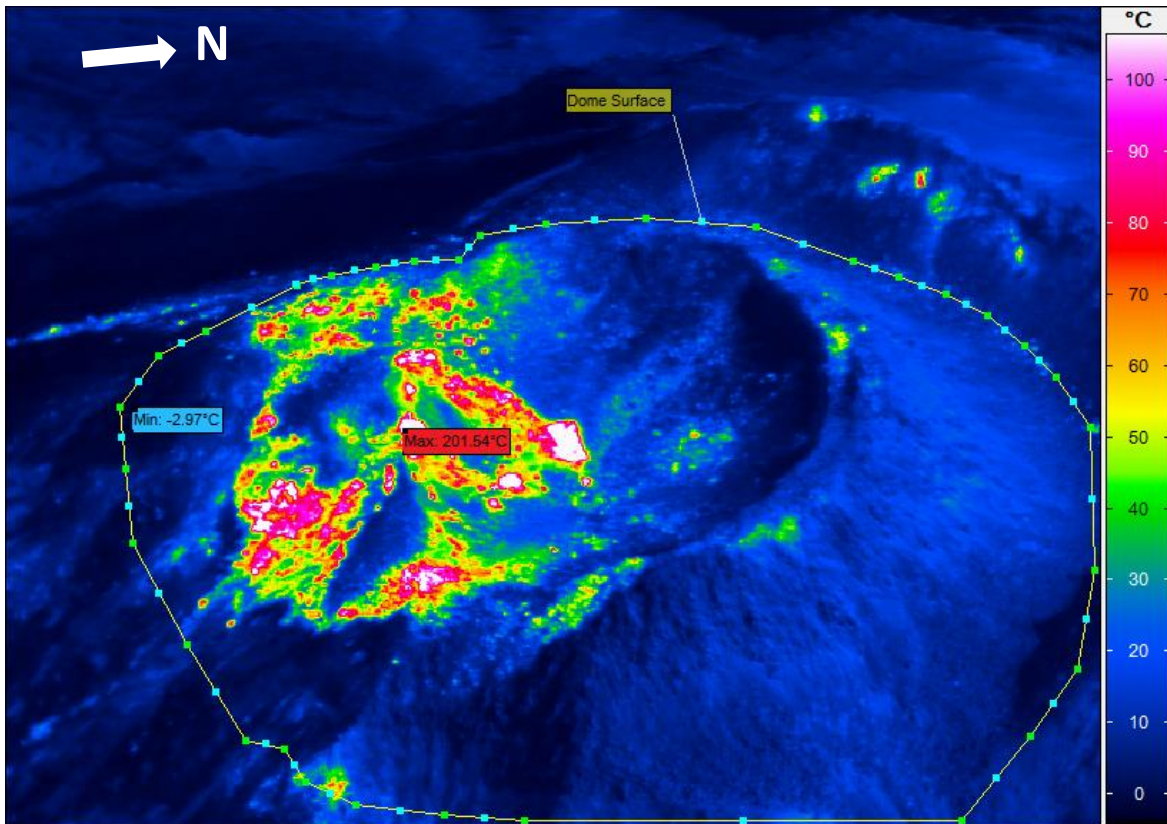

Fig. 4.6. *Thermal image from January 2013. The figure shows temperatures of the old lava dome (2007-2011).*

By February 2013, a drastic increase in temperature occurred, reaching 469 ºC (Fig. 4.7). The hottest area corresponds to the new extruded material forming the new lava dome, and is located principally at the center inside the old lava dome crater where the growth is occurring.
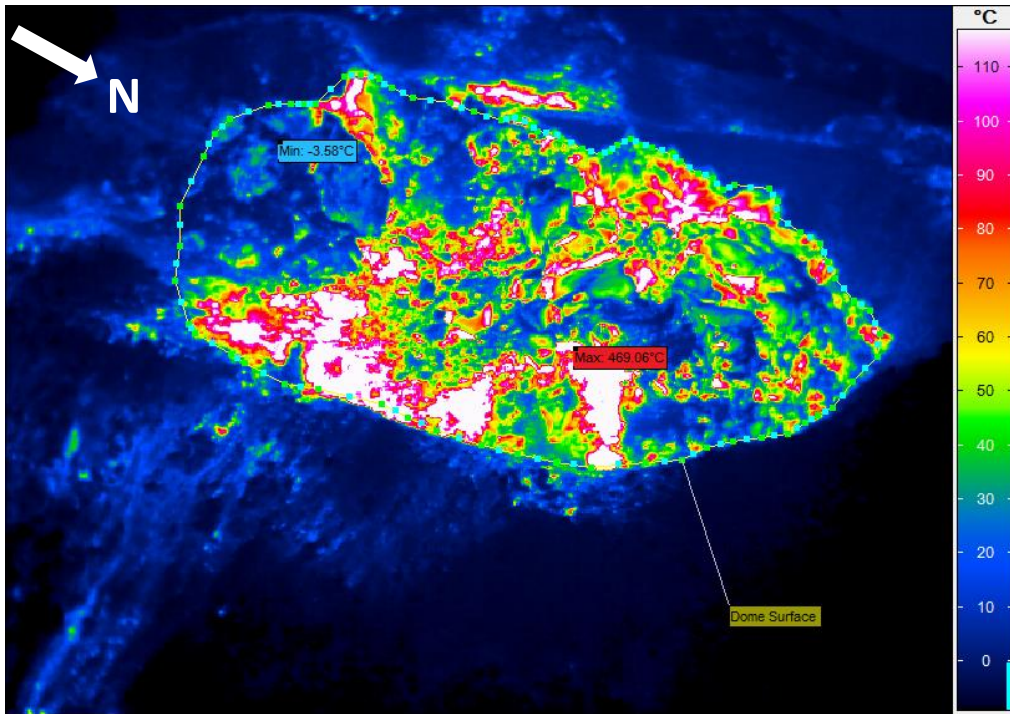
Fig. 4.7. *Thermal image from February 2013. The figure shows temperatures of the new lava dome that is starting to grow.*

In March 2013, new material was extruded at a fast rate. The hottest area (409 ℃) is located at the summit along the S flank (Fig. 4.8).
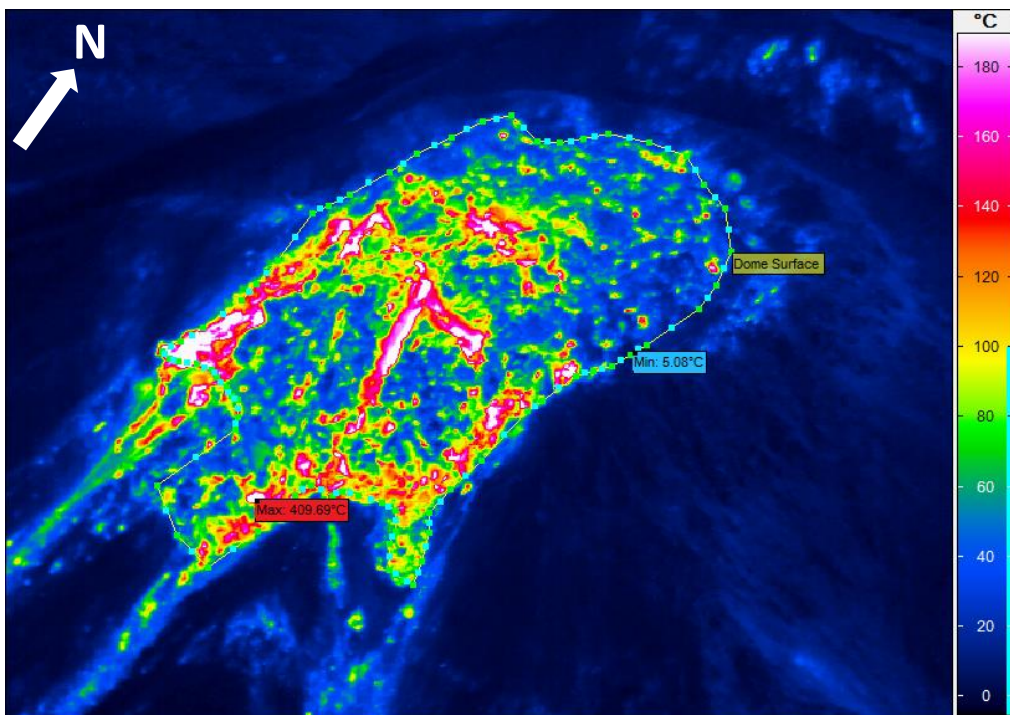
Fig. 4.8. *Thermal image from March 2013. The figure shows temperatures of the extruded material due to the growth of the new lava dome.*

During 2014, the most noticeable thermal anomaly is the high temperatures around the flanks of the old lava dome, and the maximum temperature is much lower (269 ℃) compared to March 2013 (Fig. 4.9). On the other hand, the temperatures within the crater are not homogenous, but have concentrations of hotter material on the northern flank. The bigger area of hot material is located on the upper part, and falling through the S flank, implying a quite filled crater.
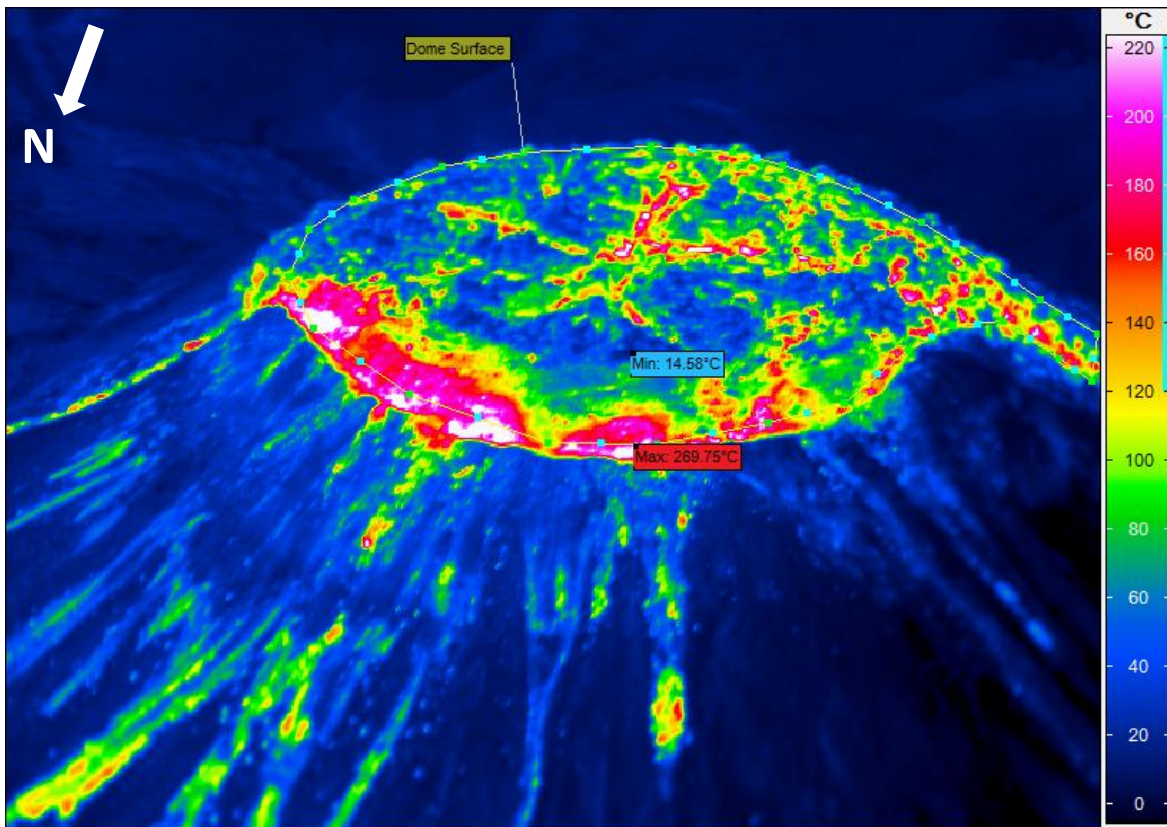

Fig. 4.9. *Thermal image from February 2014. The figure clearly shows changes in temperature around the flanks of the old lava dome, and the temperatures of the material correspond to the collapse of the new lava dome.*

Two images were chosen to represent 2015. In January 2015, we observe concentration of hottest points on the upper part of the new lava dome, and on the material overflowing the S flank. Maximum temperature recorded is 473 ℃, and it belongs to the new material and the hot gases emitted (Fig. 4.10). In September 2015, the hottest point recorded was 262 ℃, and it corresponds to the most vigorous fumaroles observed in digital photographs

(Fig. 4.3). Interestingly, temperatures are quite hot on the SW side of the inner crater where there is not much gas emission (Fig. 4.11).
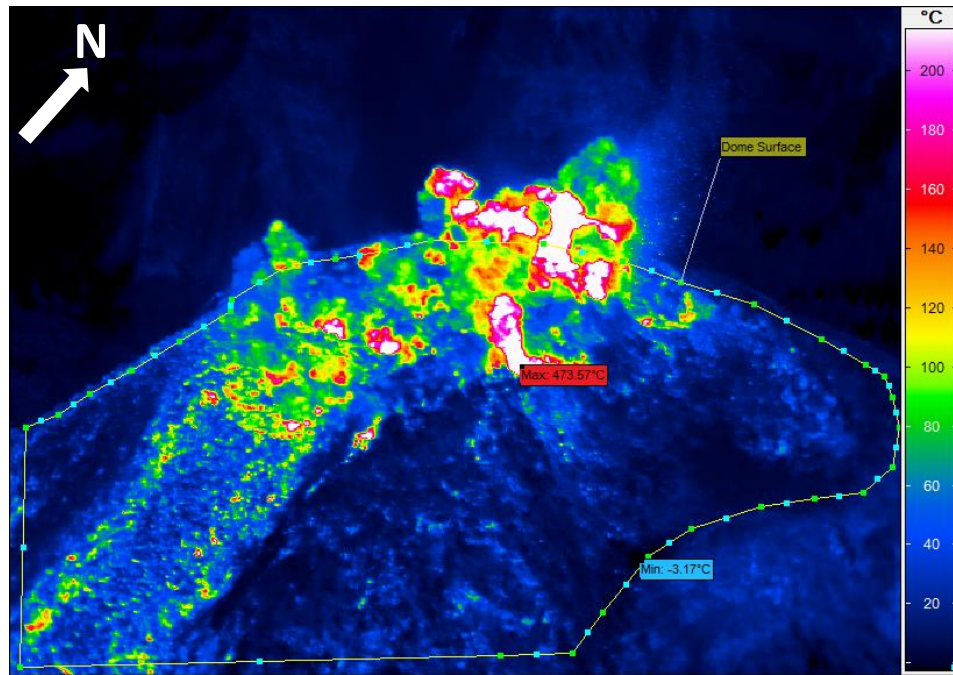

Fig. 4.10. *Thermal image from January 2015. The figure shows temperatures of the material being extruded and material from the collapse of the old dome along its flanks.*
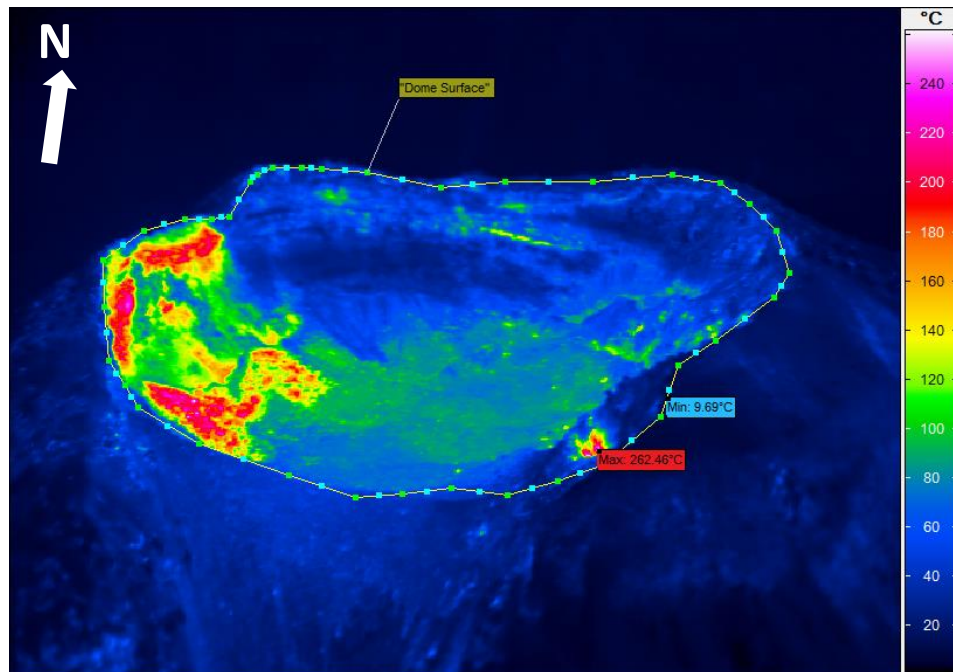

Fig. 4.11. *Thermal image from September 2015. The figure shows temperatures of the inner crater surface after the eruptive phase.*

The following images show changes in temperature during the growth phase of a new lava dome in 2016 (from Fig. 4.12 to Fig. 4.14). The year 2016 registered the highest temperatures since 2013. Maximum temperatures during the process of growth range from 330 ℃ to 530 ℃.

In March 2016, hottest points are surrounding the extruded material, and in the eastern walls of the crater (Fig. 4.12).
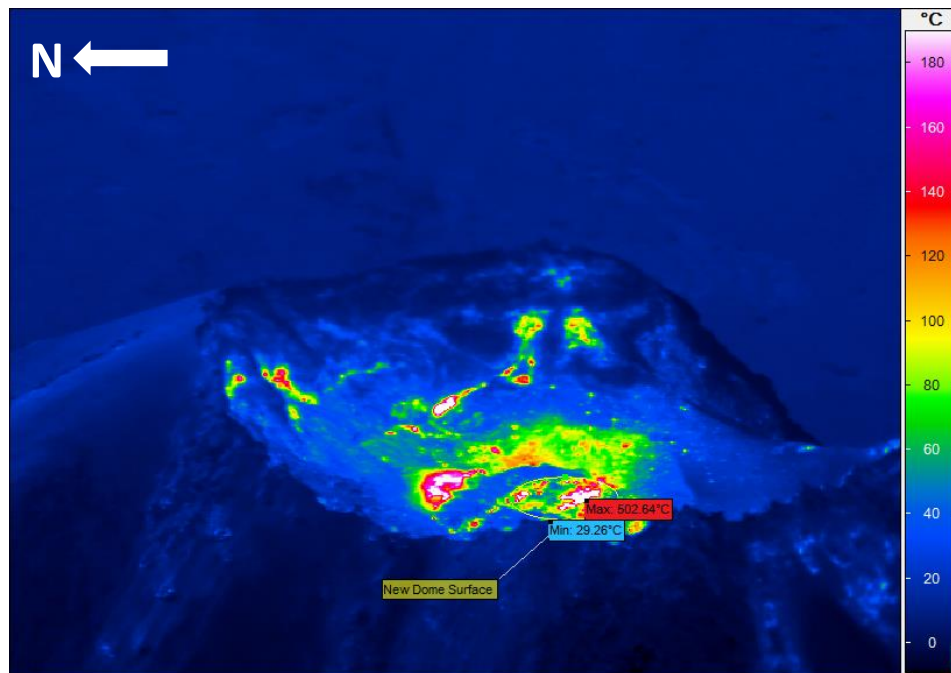

Fig. 4.12. *Thermal image from March 2016. The figure shows temperatures of the new lava dome surface.*

By May 2016, the hottest area has increased in size but decreased in temperature to 362 ℃ (Fig. 4.13).
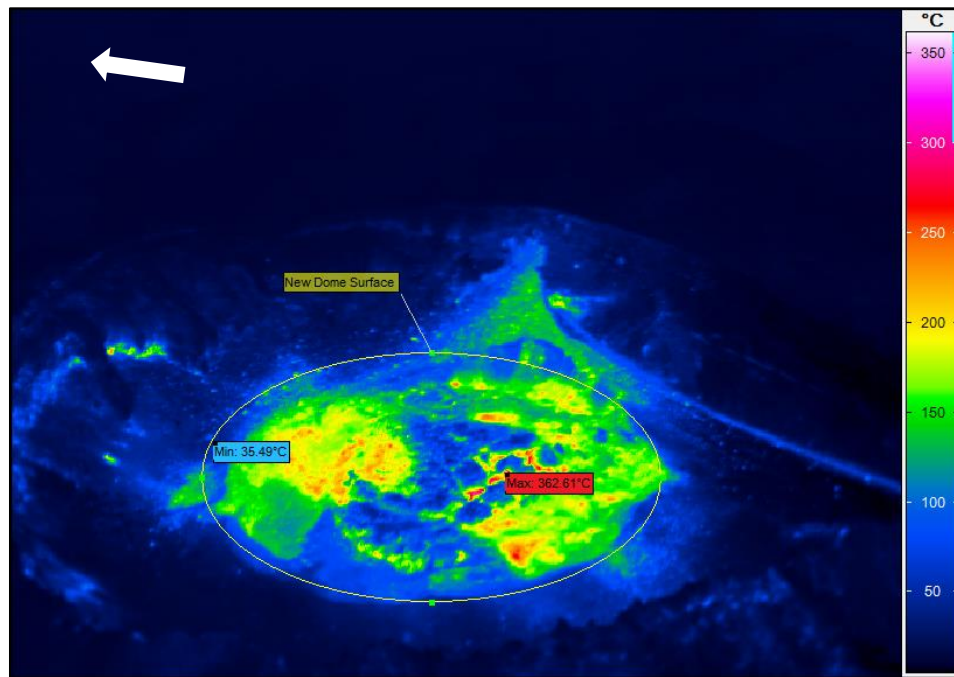
Fig. 4.13. *Thermal image from May 2016. The figure shows temperatures of the new lava dome surface.*

Finally, in October 2016, the maximum temperature recorded was 529 ºC at the center part of the extruded material within the crater. In the rest of the lava dome, temperatures are homogenous, being slightly higher at areas close to the crater rim (Fig. 4.14).
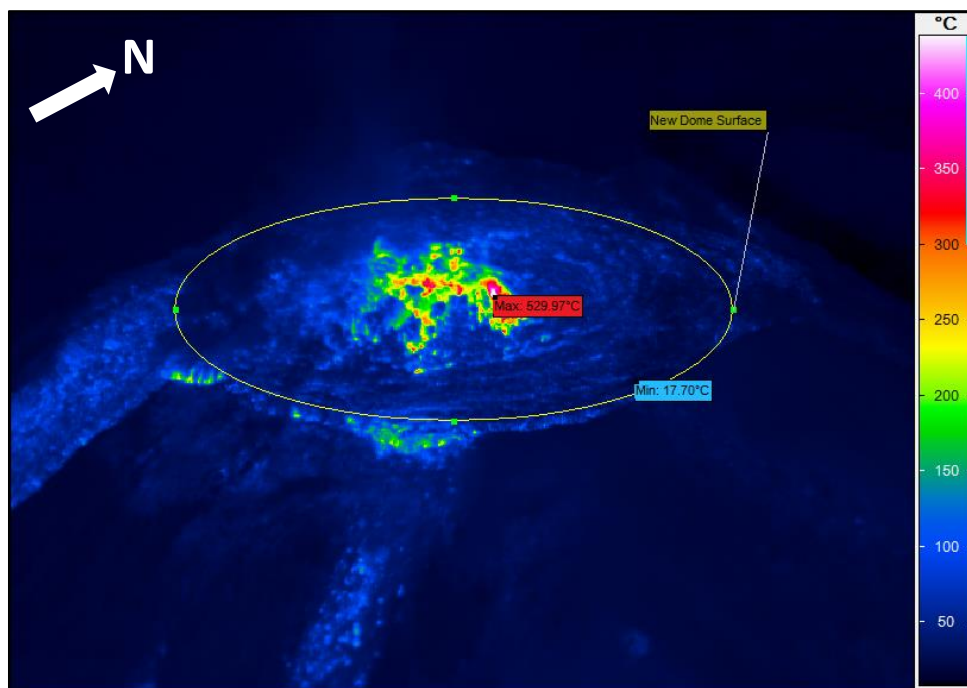

Fig. 4.14. *Thermal image from October 2016. The figure shows temperatures of the new lava dome surface.*

4.4. Effusion Rate, 2016 Lava dome

Digital photographs were used to estimate lava dome diameter and height in order to calculate dome volume through time during 2016. In addition, DRE was calculated obtaining the effusion rate during the growth process (Table 4.1).

Table 4.1. *Measured dome volumes using Inkscape for the 2016 dome growth. The table shows the calculated volume and effusion rate with and without DRE. For 16 February and 12 March volumes, we used the formula of a half-sphere. For the rest of months, volume was calculated with the formula of a frustum.*

Date	Time between measurements (days)	Measured Volume (m³)	Effusion Rate (m³/days)	Volume DRE (m³)	Effusion Rate DRE (m³/days)
16-feb	16	4.09E+03	2.56E+02	3.45E+03	2.16E+02
12-mar	25	7.53E+04	2.85E+03	6.35E+04	2.40E+03
30-apr	49	2.62E+05	3.81E+03	2.21E+05	3.21E+03
14-may	14	5.98E+05	2.40E+04	5.05E+05	2.03E+04
08-sep	117	8.28E+05	1.97E+03	6.99E+05	1.66E+03
14-oct	35	2.11E+06	3.65E+04	1.78E+06	3.08E+04
25-nov	42	2.25E+06	3.46E+03	1.90E+06	2.92E+03

The volume increase is more or less constant during the beginning of the year with a fast increase between 8 September and 14 October. During this time, the lava dome increases its volume to 1.78×10^6 m³, filling the whole crater (Fig. 4.15).
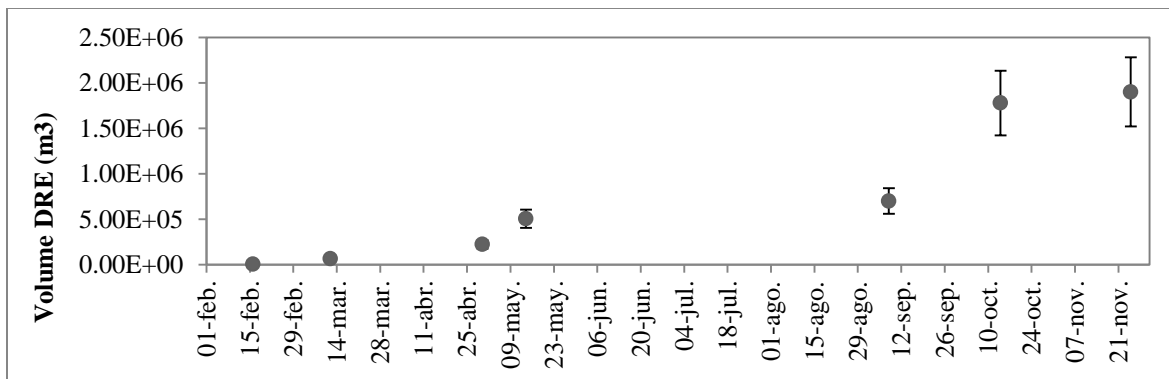

Fig. 4.15. *Changes in dome volume during 2016.*

From 16 February to 30 April, effusion rates are the lowest during the whole period of growth, reaching an average of 1.94×10^3 m³days⁻¹ (Figure 4.16). From 30 April to 14 May, the effusion rate increases rapidly to 2.03×10^4 m³days⁻¹. From 14 May to 8 September, the effusion rate decreases to 1.66×10^3 m³days⁻¹. By the 14th of October, a sharp increase in

37

effusion rate was calculated, reaching a maximum value of 3.08×10^4 m^{3}days^{-1}. It represents the filling of the whole crater. Finally, from 14 October to 25 November, the effusion rate decreases to 2.92×10^3 m^{3}days^{-1}. However, there is a less quantity of material being extruded overflowing the S flanks which underestimate our effusion rate calculation for this period.
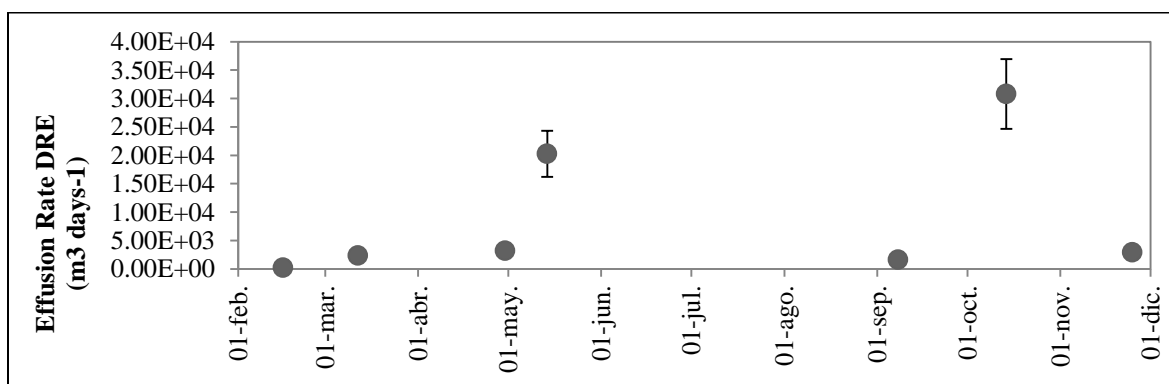

Fig. 4.16. *Effusion rate calculated for lava dome growth during 2016.*

5. Discussion

5.1. Phases of Growth, Collapse and Destruction, 2013-2016

The combination of digital and thermal images allows us to distinguish various phases of dome growth, collapse and destruction during 2013-2016. In addition, degassing and lava texture changes can be observed. In this section, phases and related changes will be described in detail.

5.1.1. Growth Phase of a New Lava Dome, February-June 2013

After 18 months of quiescence, a sequence of intermediate to small vulcanian explosions started in January 2013. In February 2013, episodes of effusive activity resulted in the growth of a new lava dome (Fig. 5.1). The new lava dome grew inside the crater of the old lava dome of 2007-2011. Thermal images suggest that the initial growth phase of the new lava dome was exogenous because the hottest material was observed on the flanks and at the top of the lava dome, highlighting extrusion at the surface of the dome (Fig. 4.7 andFig. 4.8). This material is composed principally of blocky lavas (Type I), and as the material is coming out, parts of the old lava dome fall down along the flanks. In addition, a depression

inside the crater floor of the old lava dome can be seen (Fig. 5.1). Despite this area being mostly cold, some hotter parts can be observed (Fig. 5.2). This is interesting given that no new material seems to be extruded in this area from digital images. These hot spots may thus be related to localized gas emissions through fractures in the old dome.
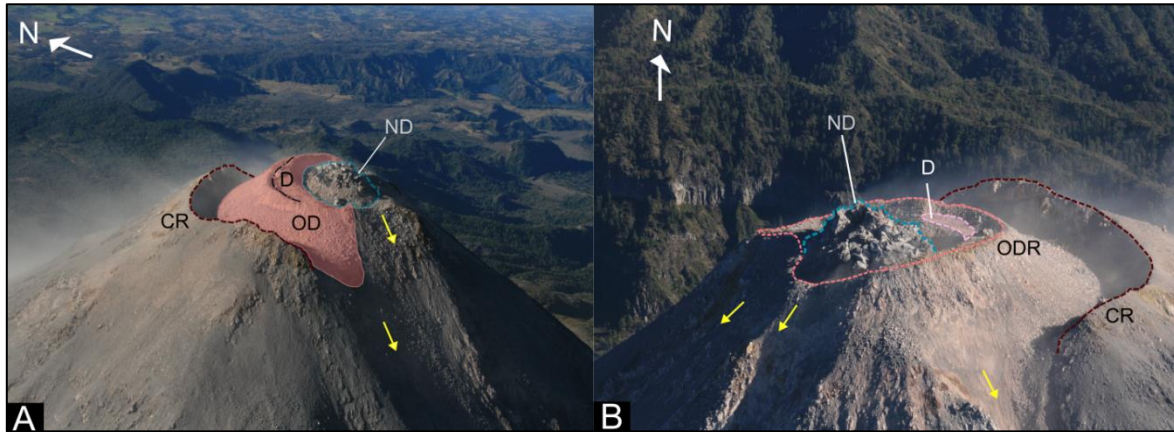

Fig. 5.1. *Initial phase of the new lava dome growth on 25th February 2013. Both figures show the principal structures of the summit at Volcán de Colima; yellow arrows indicate the direction of the material falling from different flanks of the volcano. A) D: depression; ND: new lava dome; OD: old lava dome; CR: crater rim. B) ODR: old lava dome rim.*
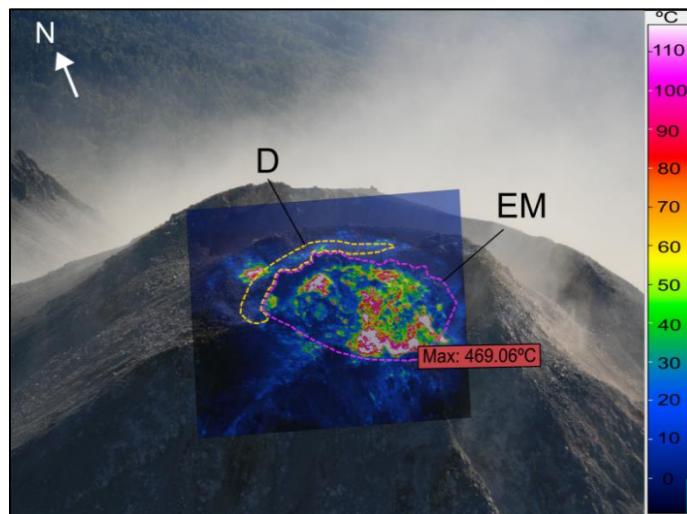

Fig. 5.2. *Thermal image from 25th February 2013. The figure shows the thermal image overlying digital photograph, and maximum temperate of the summit.*

Until March 2013, the lava dome presents exogenous growth where blocks constantly pile on top and adjacent to each other. Beginning in April 2013, endogenous growth can be observed by the way that the lava dome is being inflated (Fig. 4.1). This growth occurs at a slower rate compared to the dome formation during February-March 2013. The new lava

dome reached its highest height in June 2013 (Fig. 5.3), filling the whole crater of the old lava dome. In June 2013, the growth rate decreased and due to the steepness of the S, SW, and SE flanks, the fresh material falls by gravity. Additionally, the depression at the summit disappeared due to the inflation of the lava dome, and temperatures between 40ºC to 60ºC can be seen around the crater rim and old dome rim (Fig. 5.4). These temperatures are related with an increase in fumarolic emissions. From July to November 2013, growth rate, fumarolic emissions and rock falls seem to be constant (Fig. 4.1).
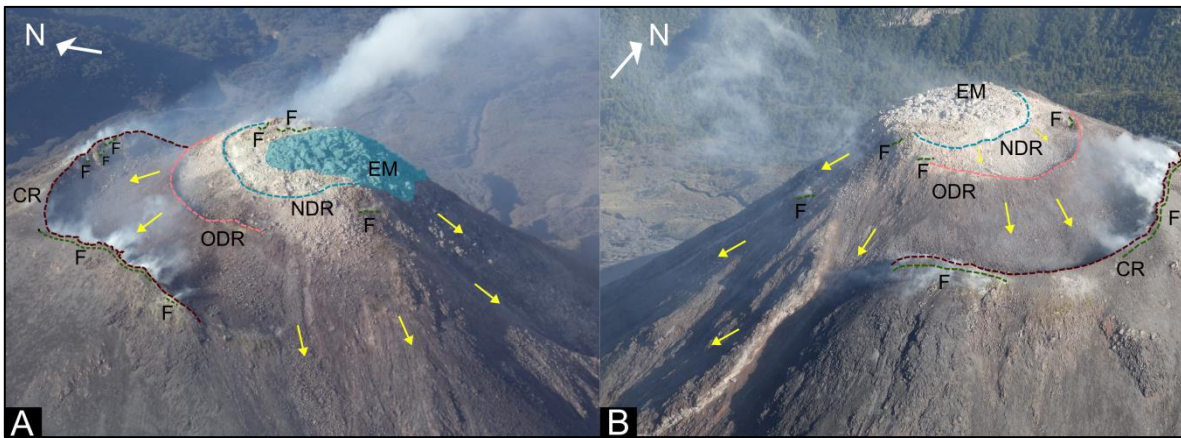

Fig. 5.3. *Digital photographs of the summit of Volcán de Colima on 20th June 2013. The figures show changes that have occurred in the Volcán de Colima summit; yellow arrows show the direction of the material falling along the flanks. **A and B**) F: fumaroles; EM: extruded material; NDR: new lava dome rim; ODR: old lava dome rim; CR: crater rim.*
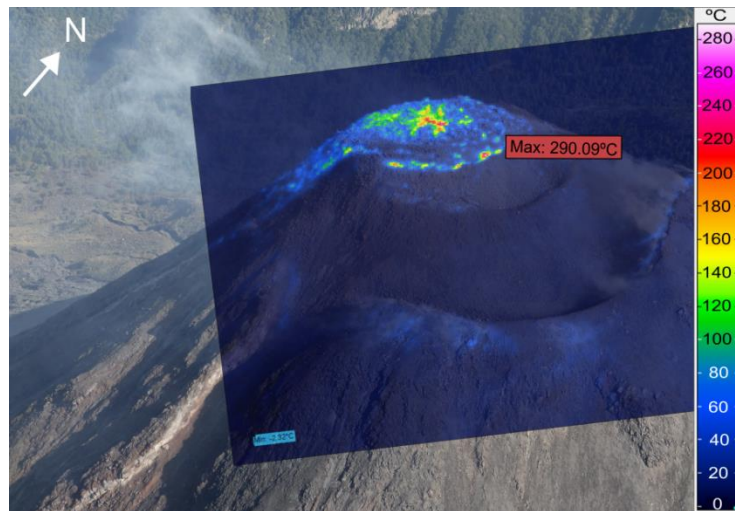

Fig. 5.4. *Thermal image from 20th June 2013. The figure shows the thermal image overlying a digital photograph, and maximum temperature at the summit.*

During the whole growth period of the new lava dome, we identify a maximum temperature at the beginning of the growth phase, reaching over 400ºC. This could be given by the exogenous growth which allowed the fresh and hot material goes out to the surface. From March onwards, temperatures and growth rate show a gradual decrease (Fig. 5.5).

Jan-Aug 2013
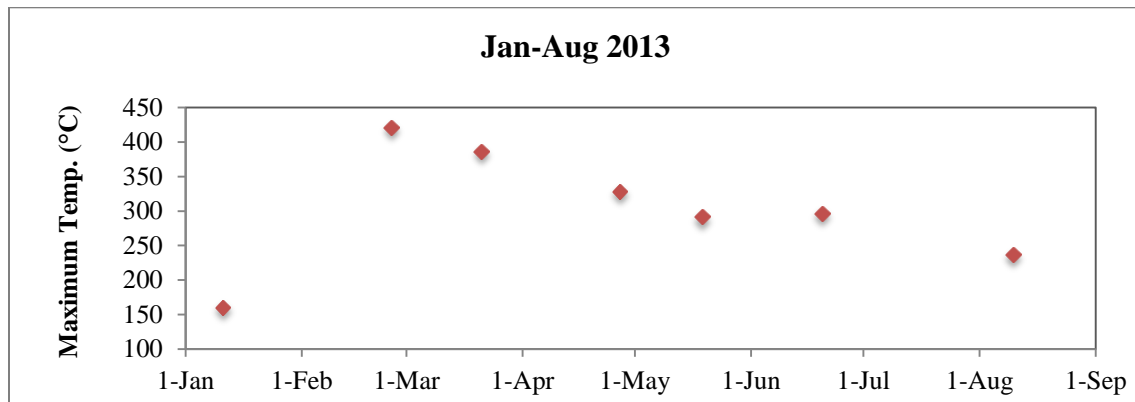
Fig. 5.5. *Maximum temperatures of the fresh material of the 2013 lava dome. The figure shows maximum temperatures reached during the growth phase of the new lava dome. Temperatures were recorded by thermal camera during monitoring flights.*

5.1.2. Collapsing Phase of the New Lava Dome, December 2013-August 2014

In December 2013, an explosive event was recorded (Fig. 5.6A). This explosive event acted as a precursor of dome collapse causing material to fall on the S, SE, and SW flanks (Fig. 5.6B). A more volatile-rich magma may be feeding the system during this period, leading to the explosive eruption when the conduit was plugged.

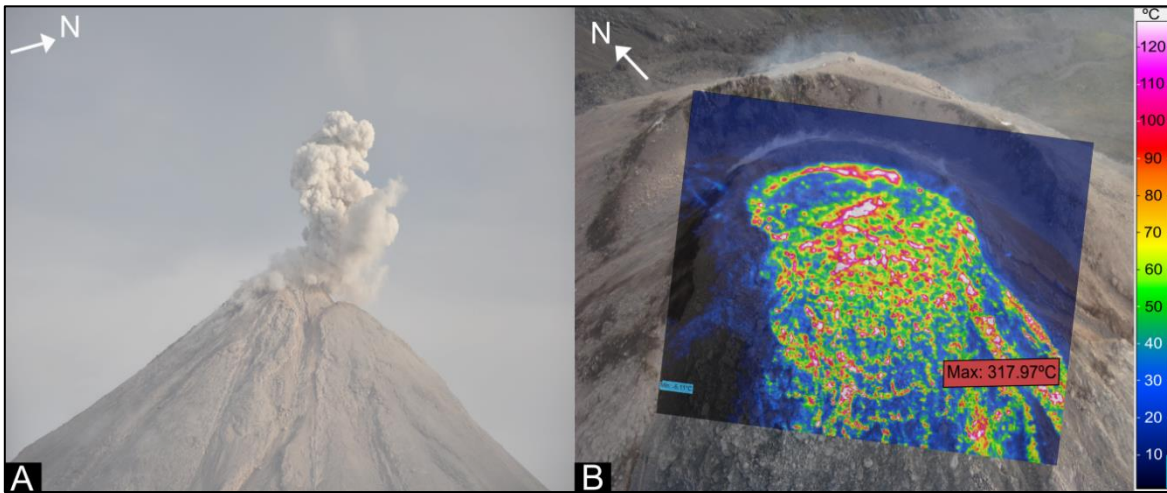**Fig. 5.6.** *Thermal image and digital photographs on 2nd December 2013. A) The image shows an explosive event at the summit of Volcán de Colima. B) Thermal image overlying digital photograph, and the maximum temperature at the summit after the explosive event.*

A depression at the summit is observed again, and erosional channels appeared on the old lava dome sides (Fig. 5.7).
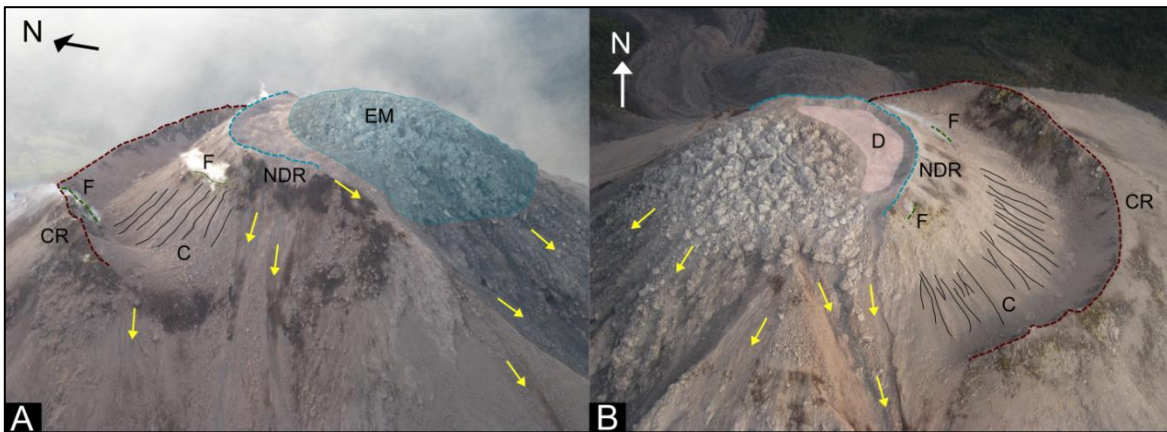

Fig. 5.7. *Digital photographs of the summit at Volcán de Colima on 2nd December 2013. The figures show changes in the summit during the first phase of the new lava dome collapse; in addition, blocky material can be clearly seen. Yellow arrows show the direction of the material falling along the flanks. A) EM: extruded material; NDR: new lava dome rim; CR: crater rim; F: fumaroles; C: erosional channels. B) D: depression.*

These structures can be due to the long-term interaction of water (meteoric and/or groundwater) with magma beneath the lava dome which results in the development and persistence of active hydrothermal systems (Ball et al., 2013). In these systems, rocks can be altered to clay minerals, weakening portions of the edifice. Additionally, it is important to know that precipitation in Volcán de Colima and the surrounding areas increased during June to November of 2013 (CONAGUA, 2013), which may explain the formation of the

depression and erosional channels by December 2013. The continuous explosive activity, and continuous growth caused the 2013 lava dome to start collapsing through the flanks (S, SE and SW flanks) as can be observed in Fig. 5.8.
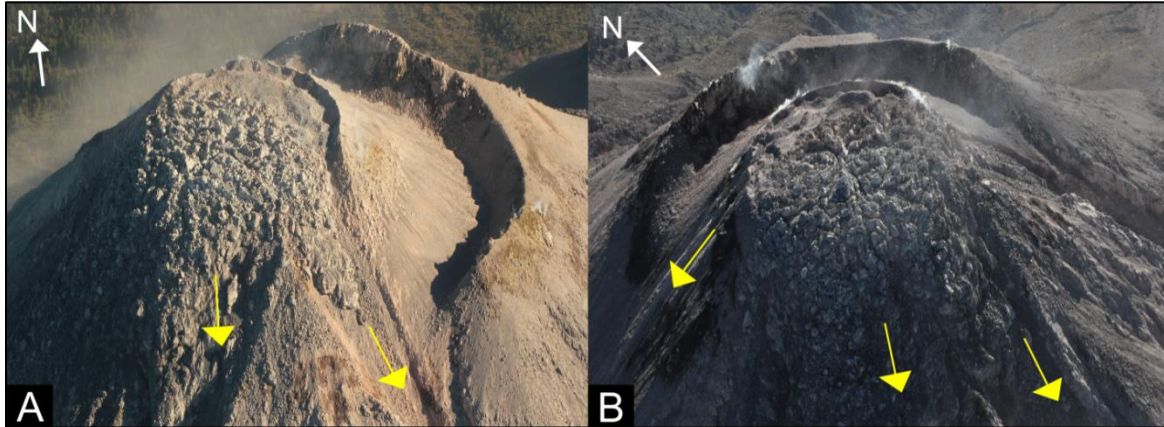

Fig. 5.8. *Digital photographs of the Summit at Volcán de Colima 2014. A) Southeastern flank of the lava dome in January 2014. B) Southwestern flank of the lava dome in February 2014. Yellow arrows show the direction of the material falling down along the flanks.*

From January to June 2014, the growth rate decreased, and the remains of the 2013 lava dome continued falling along the flanks, leaving a flat surface in the upper part of the old lava dome (Fig. 5.9).

Fig. 5.9. *Digital photograph at the summit of Volcán de Colima in June 2014. The figure shows the flat surface at the top of the old lava dome.*

In July 2014, the lava dome presented a short phase of elevated gas emissions. Fumaroles are commonly observed around the crater rim, and in the summit of the old lava dome (Fig. 5.10). The clouds of gas are white which indicate elevated water vapor content, and may be related to rainfall percolating into the hot rocks and being evaporated. This is supported by

the darker color of the flanks from July to October due to the material being wet because of the precipitation season from May to November 2014 (CONAGUA, 2014). We suggest that the increase in degassing is given by the change in gas composition to elevated water vapor content. This change could be due to an increase in magma convection rate in a shallow magmatic system induced by meteoric water penetrating volcanic edifice after heavy rainfalls (Korzhinsky et al., 2002).

Fig. 5.10. *Digital photograph from 8th July 2014. The figure shows a pronounced increase of degassing at the summit. F: fumaroles.*

In terms of temperature, high temperatures (312 ℃) were observed during December 2013 to January 2014. It can be associated with the registered explosive activity (Fig. 5.6A) providing fresh hot material to the surface (Fig. 5.7). Temperatures during the process of collapse of the new lava dome tend to be constant from February to June 2014, suggesting low rates of extruded material, and low magmatic activity.
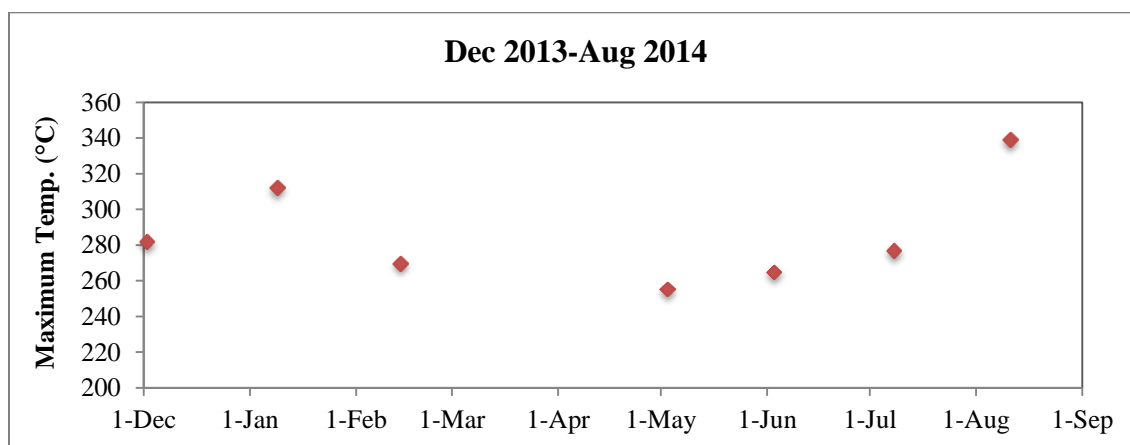
Fig. 5.11. *Maximum temperatures of the lava dome, Dec 2013-Aug 2014. The figure shows maximum temperatures per month during the collapsing phase of the new lava dome. Temperatures were recorded by thermal camera during monitoring flights.*

Starting in July 2014, it is possible to see an increase in temperatures at the surface of the dome, and the southern east side of the crater rim, which could be associated with the increase of degassing related to rainfall percolating into the hot rocks and being evaporated (Fig. 5.10). Finally, an increase in temperature (339 °C) towards August is likely related with newly extruded material of Type I on the western part of the upper lava dome surface.

Lastly, thirteen major lahars were recorded from two monitoring stations from June to September, the local rainy season, with no reported damage (Global Volcanism Program, 2015). These lahars may be related to the collapse of the lava dome that occurred from December 2013 to July 2014, providing fresh and loose material that is easy to remobilize during heavy rain events.

5.1.3. Destruction Phase of the Old Lava Dome, September 2014-December 2015.

At the beginning of this phase, the 2013 lava dome is not visible anymore. The major part of the blocky material forming the lava dome has completely fallen down the flanks, and other portions of it are weathered to fine material due to hydrothermal alteration caused by degassing of water vapor, and acidic gases. However, there is no evidence of a complete disappearance of the 2013 lava dome due to the presence of gas clouds, which make observation of the summit difficult (Fig. 5.12).

Fig. 5.12. *Digital photograph from 20th of September 2014. The figure shows newly extruded material falling along the S flank, and gas clouds which make observation difficult.*

A major explosive event occurred in September 2014, causing new extruded material to go down the SW and S flanks (Fig. 5.12). The newly extruded material had a different texture than lavas extruded in previous phases. This new material is composed of smaller black blocks of type II (Fig. 4.5B). Explosive activity leaves the vent free which may allow hotter material to reach the surface faster. Thus, magma is less viscous due to the highest temperatures, and it allows the new extruded material to overflow the summit easily compared to the previous more viscous material (Type I). By late November 2014, it is possible to see notable changes in the volcano summit (Fig. 5.13). Newly extruded material and portions of the old lava dome edifice almost fill the principal crater of the volcano.
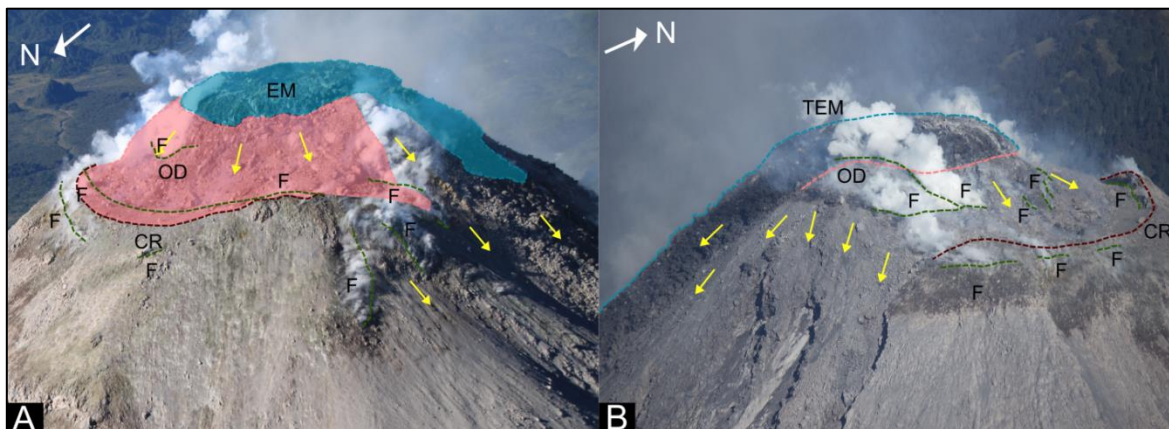
Fig. 5.13. *Digital photographs of the summit at Volcán de Colima on 26th November 2014. The figures show the newly extruded material and the collapsing of the old lava dome along the flanks; yellow arrows show the direction of the material falling from the summit. A) EM: extruded material; OD: old lava dome; CR: crater rim; F: fumaroles. B) TEM: top of the new extruded material.*

5.1.3.1. Increase of Explosive Activity

During November and December 2014, Volcán de Colima presented an explosive eruptive sequence which destroyed the whole dome formed at the beginning of the eruptive episode in 2013 (Global Volcanism Program, 2015). The strongest eruptions were recorded on 21st and 30th November. Both eruptions were vulcanian (Fig. 5.14). The eruptive sequence was accompanied by ash plumes, pyroclastic density currents, dome destruction and high concentration of gases at the summit (Fig. 5.15). Given that this sequence took place during the dry season, we suggest that the increase of gases may be of magmatic origin. A more volatile-rich magma may be feeding the system during this period, leading to an explosive eruption if the conduit is plugged and to intense degassing in open-conduit conditions.

Fig. 5.14. *Volcán de Colima's eruption on 30th November 2014. The resulting plume rose to ~5 km. Taken from Global Volcanism Program (2015)*
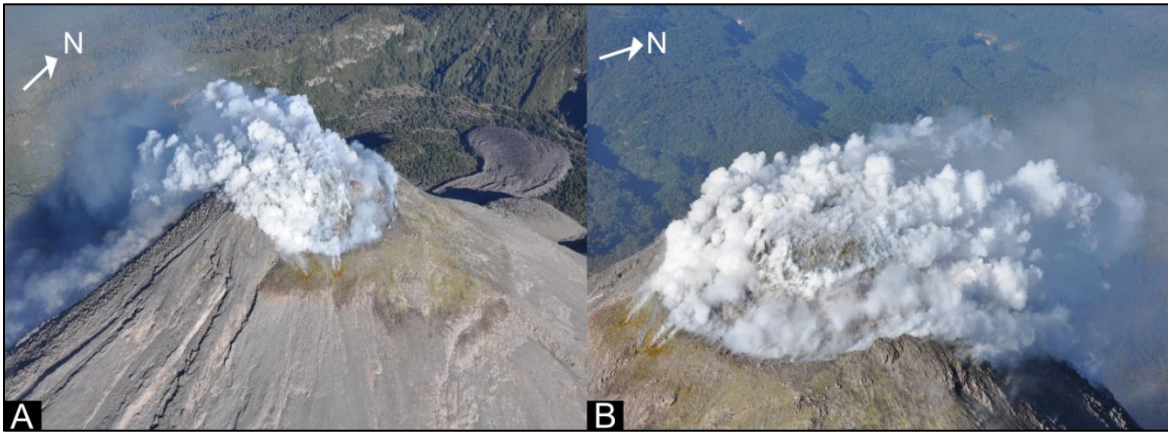
Fig. 5.15. *Digital photographs of the summit at Volcán de Colima on 16th December 2014. The figure shows degassing at the summit.*

Explosive vulcanian activity during 2015 was intense, associated with rock falls, lava flows and PDCs (Fig. 5.16). Ash plumes produced during the most explosive events reached heights over 7 km, and often reached distances of 150 kilometers or more from the volcano. Two significant eruptions happened during this year, on 21st January and 10th July (Global Volcanism Program, 2015).
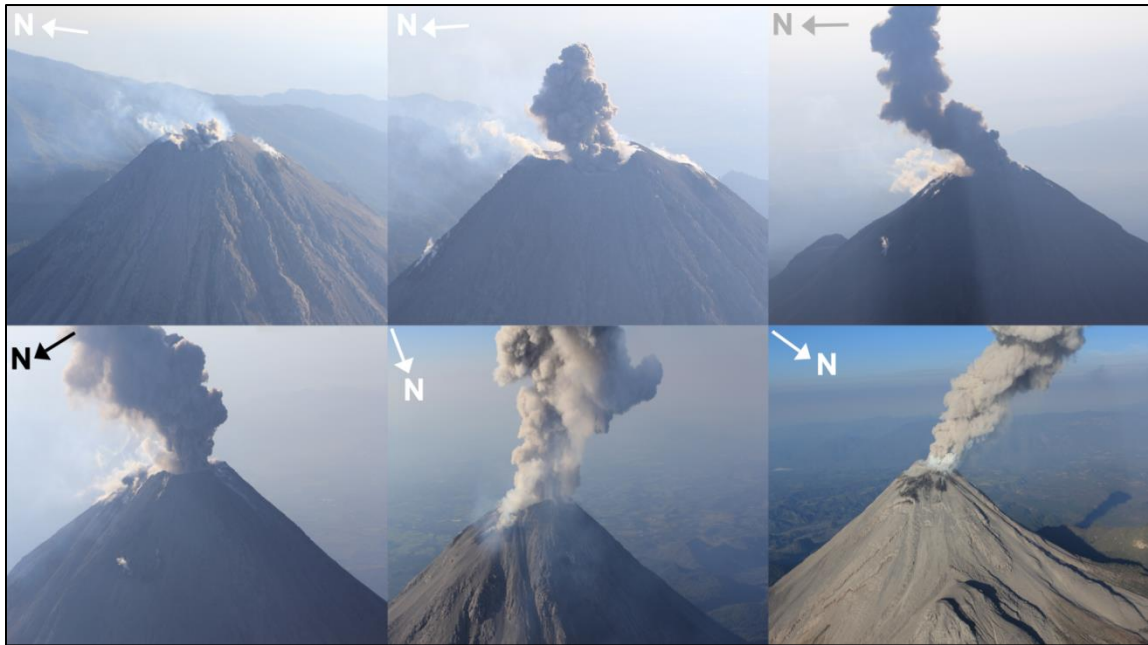
Fig. 5.16. *Vulcanian eruption recorded on 31st March 2015 at Volcán de Colima.*

By January 2015, the old lava dome and the whole summit have changed their morphology. As we can see in Fig. 5.17, the summit of the old lava dome has collapsed, filling its whole talus edge.

Fig. 5.17. *Digital photographs showing the changes in the summit area between November 2014 and January 2015 due to explosive activity. Black dashed line indicates the crater rim. White arrows show the north.*

The extruded material during the destruction phase presents a variety of textures, being more blocky and bigger in size in the upper rounded part of the summit (Fig. 5.18). The darker material along the flanks possibly extruded with the first pulse of magma, followed by the light colored blocky material, and finally in January the darker part at the center of the summit was filled by magma. This indicates exogenous growth, with the newly extruded lava being emplaced at the center while older material forms a circle around it. If the dome continues to extrude magma and inflate, this process will repeat itself and additional concentric layers can be emplaced (Calder et al., 2015).
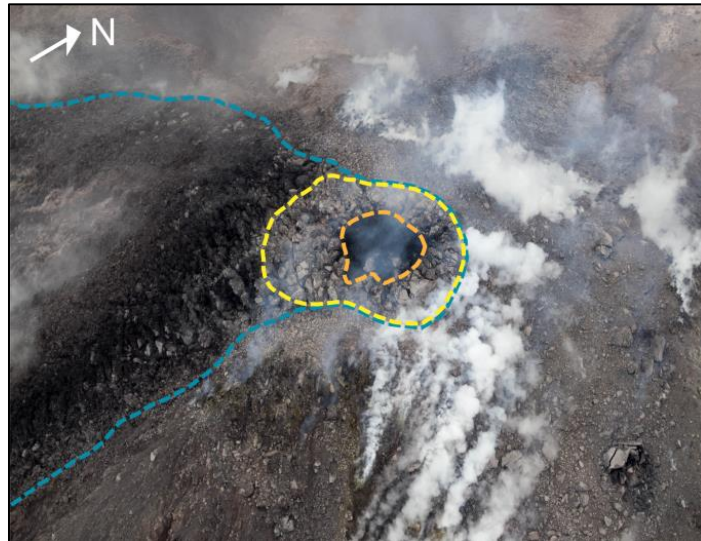
**Fig. 5.18.** *Digital photograph of the summit at Volcán de Colima on 4th January 2015. The figure shows abrupt changes of the whole summit, and degassing before 21st January eruption. Light blue dashed line: first pulse of magma; Yellow dashes line: blocky material extruded (intermediate pulse); Orange dashed line: last pulse of magma.*

Since February 2015, the summit of the old dome area formed a depression. It looks completely different because the blocky extruded material and the top of the old lava dome have disappeared. The crater is covered by a layer of fine material with small depressions in different parts of the inner crater (Fig. 5.19A).
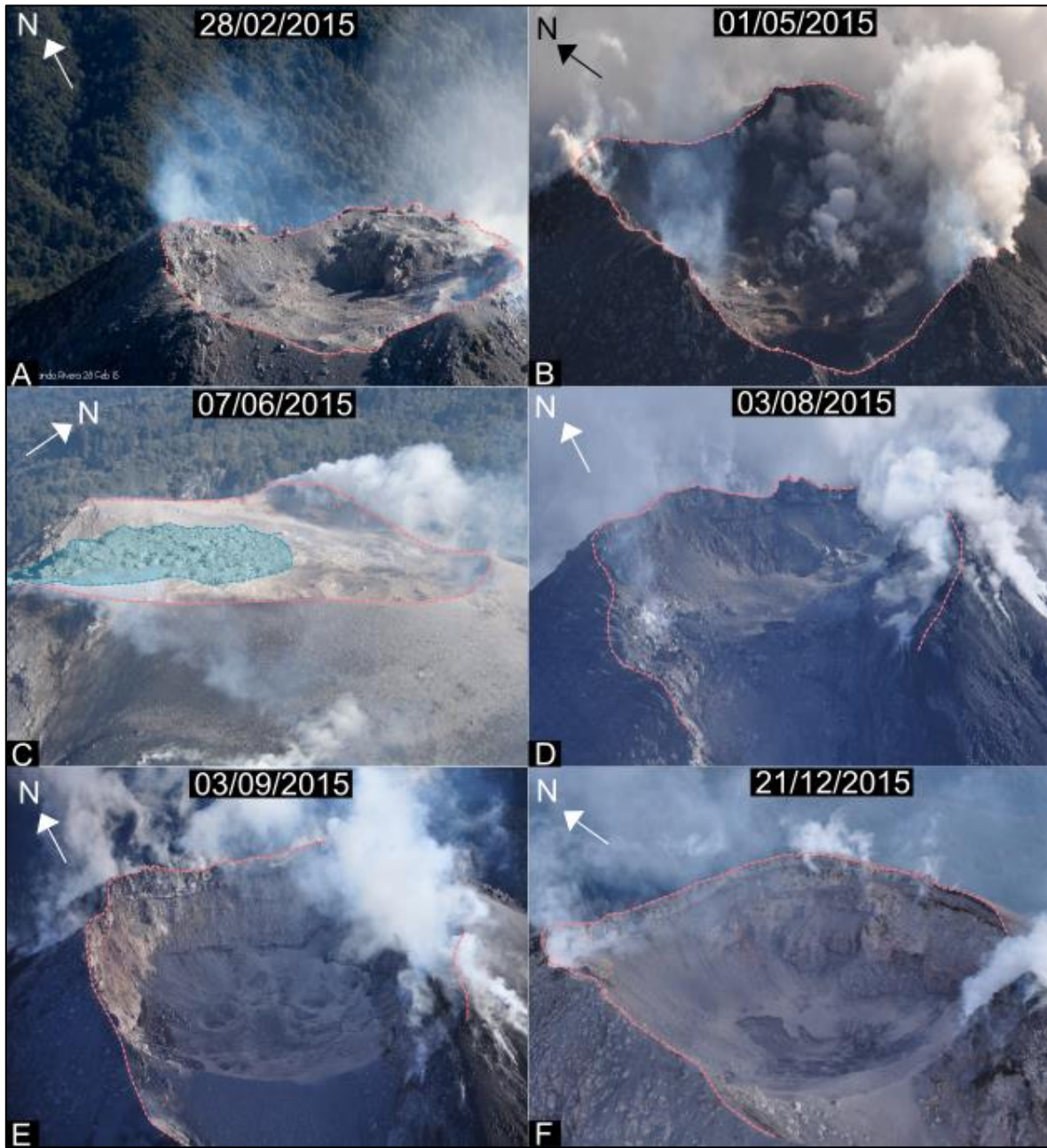
Fig. 5.19. *Digital photographs of the summit during 2015. All figures show changes at the summit during 2015; pink dashed line shows the crater rim, and light blue polygon shows extruded material. A) Depression formed after the lava dome has been destroyed. B) The crater floor after being exposed by 31ˢᵗ March eruption. C) New lava dome emplacement. D) Inner crater after June lava dome was erupted by July 10th-11th eruption. E) Crater after being highly altered by acidic gases, stratigraphy of the inner walls is visible. F) Fine material falling along the inner crater walls. In addition, the crater floor is subsiding, forming a concave shape.*

All those changes occurred after the 21ˢᵗ of January 2015 vulcanian eruption which removed the dome material, leaving the crater almost empty. Acidic gases emitted during this eruption altered the inner crater walls, and blocky lavas to fine material. On 31ˢᵗ March 2015, a small vulcanian eruption was registered. This was the last event that leaved the

crater completely empty with a concave shape. From April to May 2015, low activity, degassing and alteration of the inner crater walls to finer material can be seen (Fig. 5.19B). Beginning in June 2015, fast emplacement of a new lava dome is observed (Fig. 5.19C). The crater floor is covered by Type I material (Fig. 4.5C), and sandy material which fills some depressions inside the crater. Due to the crater being almost completely filled, with little extruded material visible, we suggest that the emplacement of the dome started in May with a fast exogenous growth followed by an endogenous process. According to Reyes-Dávila et al. (2016), during July 10th-11th 2015, Volcán de Colima had the most intense eruptive phase since its 1913 AD Plinian eruption (Fig. 5.20). This event presented two phases of dome collapse. The second one was the largest, and produced a series of PDCs that were mostly channelized by the Montegrande and San Antonio ravines (Fig. 2.8), reaching a distance of approximately 10.3 km. The eruption and dome collapse formed an amphitheater-shaped crater open towards the south (Fig. 5.19D).

Fig. 5.20. *Digital photograph of the second PDCs on July 11th, 2015, taken from the east. The absence of an eruptive column rising vertically is clear from this picture which suggests it is not a vulcanian eruption, but a pyroclastic flow sweeps down the flank due to a Pelean eruption. Taken from Reyes-Dávila et al. (2016).*

For the rest of 2015, the intensity of the explosions decreased, but ash plumes were emitted nearly every day until the end of the year. These explosions excavated parts of the crater exposing its inner walls, and blocky material was replaced by finer material. This might be due to removal of the blocky material during explosive events, coupled with alteration due to the acidic gases being constantly emitted, as well as the blanketing of ash following the

explosions (Fig. 5.19D to F). Finally, weak fumarolic activity was present with gas plumes which rose from vents outside the crater, and in the SE part within the crater.

In terms of temperature, the phase of destruction of the old lava dome includes an important variation in temperature (Fig. 5.21). We first observe a decrease in temperature from August until October 2014 due to a low activity phase in the volcano. Consequently, it is possible to see a cyclic increase-decrease of temperature associated with the most explosive phase during earlier November 2014 to March 2015. In that period, abrupt changes in morphology also occurred due to the vulcanian eruptions. In June 2015, an increase in temperatures can be related to the lava dome emplacement and the beginning of the most intense eruptive phase since 1913. Increased heat flow associated with the ascent of magma toward the surface is clearly observed. However, temperatures in June are quite low compared to the November-January 2015 registered temperatures. This could be due to the strong influence of the effusive activity (Nov-Jan) which constantly extruded fresh and hot material at the surface. After that, an eruption in January removed the entire lava dome, and temperatures at the surface cooled rapidly by radiative heat loss (Aries et al., 2001).
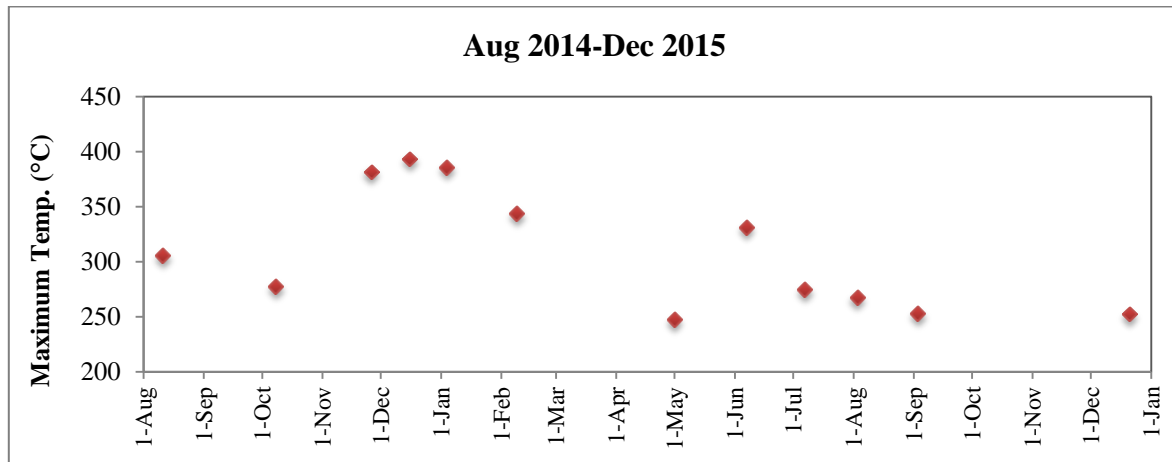
Fig. 5.21. *Maximum temperatures of the fresh material, lava dome and the crater, Aug 2014 - Dec 2015. The figure shows maximum temperatures per month during the collapsing phase of the old lava dome. Temperatures were recorded by thermal camera during monitoring flights*.

Finally, following the July 2015 eruption, temperatures decreased steadily until the end of the year because of the fast cooling of the surface. It may be related with the endogenous growth which does not allow the extrusion of fresh material to the surface.

5.1.4. Growth Phase of a New Lava Dome January 2016-December 2016

In 2016, we can observe that the old dome has been completely destroyed by the last episodes of explosive activity (Fig. 5.22).
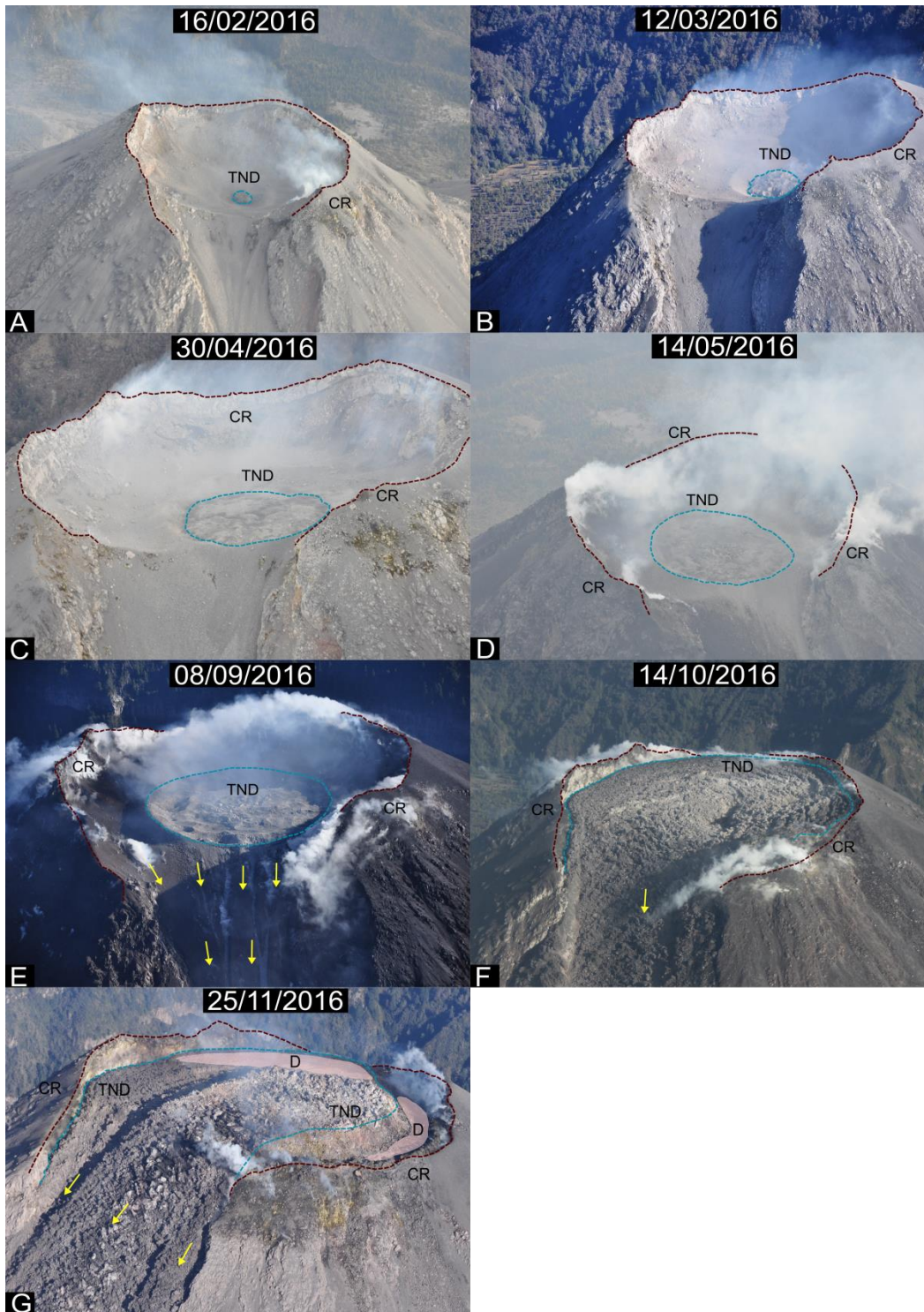
Fig. 5.22. *Growing phase of a new lava dome during 2016. Figures show morphological changes of the summit during the growing phase of a new lava dome; yellow arrows show direction of the material flow. CR: crater rim; TND: top of the new lava dome; D: depression.*

Since January 2016, Volcán de Colima was very active, presenting constant ash emissions. In February 2016, a new lava dome started growing (Fig. 5.22A to G), with a constant rate of growth until late April, followed by a rapidly increasing effusion rate until 14 May (Fig. 4.16). After that, activity and the effusion rate decreased until September, although multiple explosions with ash plumes still took place almost weekly during that period. The occurrence of explosive events during dome-forming periods of low effusion rates can be explained by the formation of a solidified dome cap or the attachment of magma to conduit walls, which increases pressurization in the conduit (Ogburn et al., 2015).

From October to November 2016, the lava dome overflowed the crater rim, producing a slowly moving lava flow goes down the SW flank (Fig. 5.22F) (Global Volcanism Program, 2017). In addition, beginning in October 2016 the extruded material has a texture of Type III (Fig. 4.5D), but by latest November 2016, the texture of the extruded material is of Type I (Fig. 4.5E). This could represent a change in the magma composition and temperature.

From September to October, the dome rate of growth increased, filling quite fast the whole crater, and reaching the maximum effusion rate of the whole growth period (3.08×10^4 $m^3 days^{-1}$) (Fig. 4.16).

In November, the rate of growth decreased, and the inflation process started. Although, a few newly material is being extruded, from late September to November, there is a continuous loss of material flowing down the S flank which underestimates our effusion rate calculation.

Temperatures during the growth phase of the new lava dome increase with time, reaching a maximum temperature of 511 ºC on 14th of October (Fig. 5.23). The increase of temperature in February is associated with emission of hot lava at the surface at the beginning of the lava dome growth. Another increase of temperature can be seen in April. It could be given by a fast magma output which rapidly increases the diameter of the lava dome (Fig. 5.22C and D).

From late April to September 2016, an endogenous growth is defined by the low extrusion rate of material and the inflation of the dome. Later, from September to October, there is a

fast extrusion of material, following an exogenous growth that filled the whole crater (Fig. 5.22E and F). It could explain the highest temperature reached on 14 October (Fig. 4.16). Increasing temperature produces less viscous magma, which is able to flow easier through the conduit causing an increase of discharge rate.
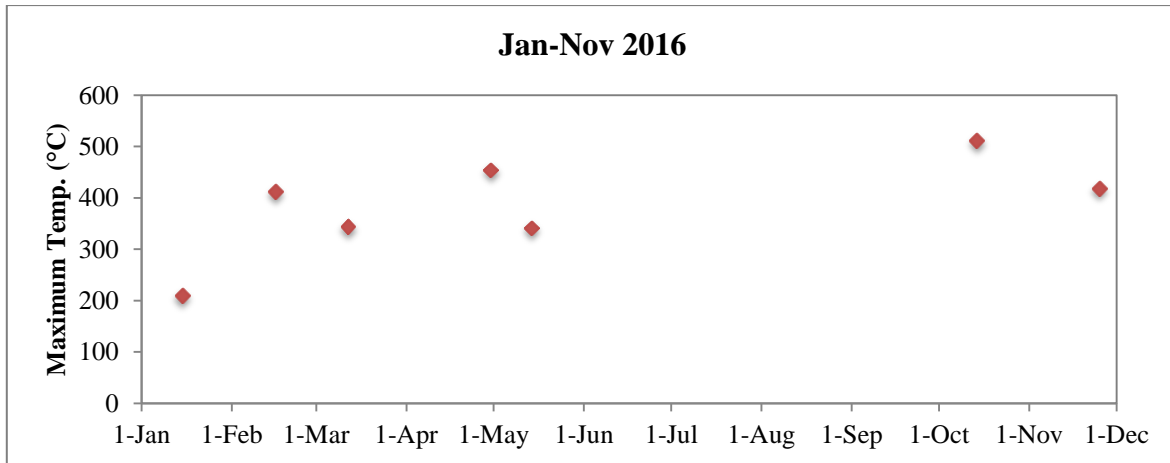

Fig. 5.23. *Maximum temperatures of the extruded material forming the new lava dome during 2016. The figure shows maximum temperatures per month during the growth phase of the new lava dome. Temperatures were recorded by thermal camera during monitoring flights.*

According to our results of effusion rates and temperatures, we suggest that they are related to changes in lava texture. Thus, growth of the 2016 lava dome has been divided into four stages, summarized in Fig. 5.24. These stages depend on the effusion rate, temperature, type of extruded material, and process of growth (exogenous or endogenous).

Fig. 5.24. *Stages of lave dome growth in 2016, according to calculated effusion rates and observed textures.*

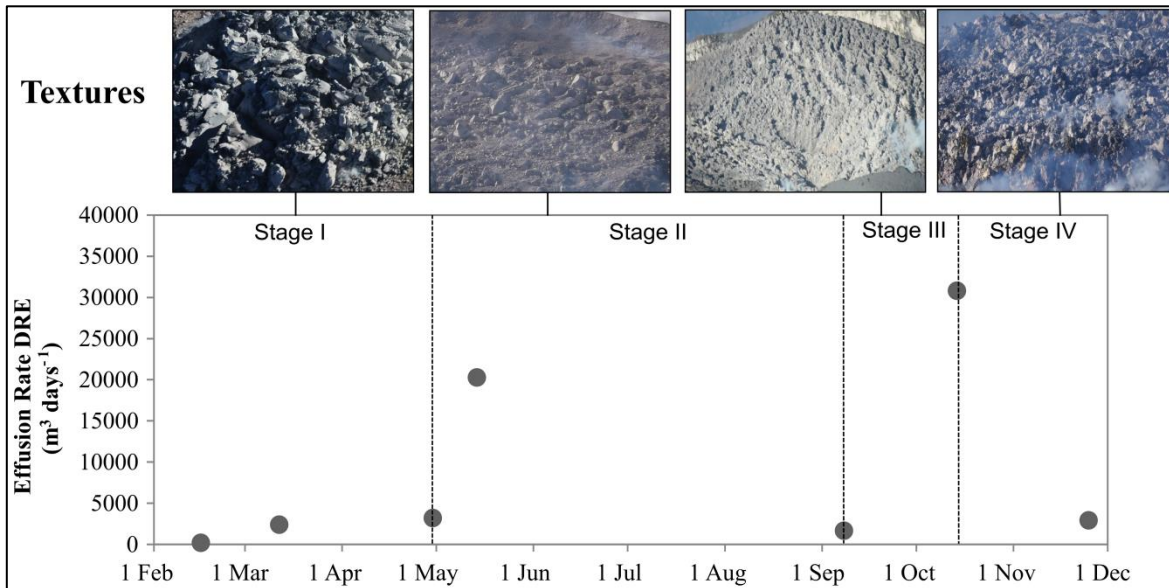Stage I is characterized by a maximum effusion rate of ~3.21×10^3 m^{3}days^{-1} (Table 4.1), average temperature of ~404 ºC, extruded material of Type I and exogenous growth. Stage II is defined by a higher effusion rate between May and June reaching the highest value in 14 May (~2.03×10^4 m^{3}days^{-1}), and a lower extrusion rate between May and September (~1.66×10^3 m^{3}days^{-1}) (Table 4.1). Temperatures reached ~341 ºC, and the extruded material belongs to Type I. The lava dome has an endogenous growth during this stage. Stage III is characterized by the highest effusion rate during the whole period (~3.08×10^4 m^{3}days^{-1}), the highest temperatures reaching ~511ºC, less viscous extruded material of Type III, and exogenous growth. Finally, stage IV is defined by a decrease of effusion rate (~2.92×10^3 m^{3}days^{-1}), and a continuous loss of material falling down the flanks. Temperatures reached ~418 ºC; Type I material was extruded and exogenous growth occurred. According to Sparks et al. (1998), lower effusion rates (Stages I and IV) can be explained by degassed and highly viscous lavas, which slows down the flow rate and can restrict the conduit by solidification reducing the discharge rate. In addition, temperatures during these stages are the lowest which can be related with cooler, more viscous lavas. On the other hand, high extrusion rates (Stages II and III) during shorter periods of time can be associated with ascent of increasingly fluid and gas-rich magma (Ryan et al., 2010; Sparks et al., 1998). Higher surface temperatures of the extruded material during this period agree with emplacement of less viscous lavas.

5.1.5. Eruptive Chronology

Using all the information extracted from digital and thermal images, we define the following growth processes, eruption phases and lava texture changes. During 2013-2016, Volcán de Colima presented different phases of lava dome growth (Fig. 5.25). The growth processes for both the 2013 and 2016 lava domes began with lava extrusion, followed by mainly endogenous growth, characterized by inflation of previously erupted lavas. Consequently, these lavas fall along the flanks, and changes in the textures of extruded material are observed, due to changes in composition, temperature and behavior. The endogenous growth gradually slows down but persists until an eruption or collapse occurs.

Based on the eruptive activity that occurred at Volcán de Colima, we divided the 2013-2016 period into phases (Fig. 5.25). Volcán de Colima is characterized by its effusive activity (lava domes), but also its explosive activity (Vulcanian and Pelean eruptions). Between these phases, there is a transition phase between effusive-explosive, explosive-explosive, and effusive-effusive events where the volcano does not present activity. During this quiescent period, the volcano keeps a constant low volcanic activity.

In order to determine the type of eruption for the all of the processes that occurred during 2013-2016, the following statements were considered:

- Growth of a lava dome is a common style of effusive eruption which can occur before or after explosive events. In addition, the magma discharge and effusion rates are much smaller than in explosive events, and can continue at a low rate for long durations (Pallister et al., 2013).
- Explosive eruptions include high emission rates but short duration impacts (Nakada et al., 2016).
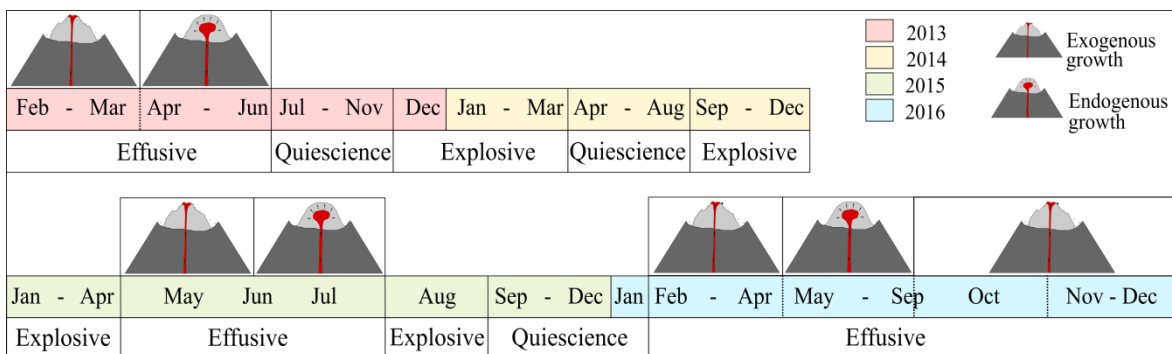
Fig. 5.25. *Sketch showing the type of eruptive activity and growth process in chronological order of Volcán de Colima from 2013 to 2016.*

6. Conclusions

Lava domes forming at Volcán de Colima show growth processes that evolve with time. For the 2013 and 2016 lava domes, we observed that they started with exogenous growth, and then changed to endogenous growth, with a continuous fall of material around the flanks. In addition, during the endogenous growth period there were intermittent short periods of extrusion of material overflowing the crater down the flanks.

Volcán de Colima is characterized principally by its effusive eruptive activity. However, during the period 2013-2016, it experienced different eruptive phases: effusive which is recognized by the lava dome formation, and explosive which is defined by variable sized vulcanian eruptions, and one Pelean eruption that destroyed the whole 2007-2010 lava dome. Between these phases, periods of quiescence were recognized, characterized by low activity and lack of morphological changes in digital images.

The highest temperatures, between ~350 and ~500 ºC, are related to the preliminary phase of lava dome growth, and strong explosive events. During the other phases, average temperatures range from ~200 to ~350 ºC.

Finally, using temperatures, type of extruded material and effusion rates calculated, we defined four stages for the lava dome growth of 2016. We found that the maximum effusion rate in this period was ~$3.08{\times}10^4$ m^3days^{-1}, related to increased temperature, and extruded material of type III, which is unique to this 2016 growth process.

For future work, we recommend to continue to monitor these changes. Furthermore, combining these analyses with geochemical studies would allow one to have a better idea of the magma composition, and thereby more accurate estimates of the conditions such as depth and temperature at which these lavas are being formed. Additionally, taking good GPS points during monitoring flights will help to provide more accurate measurements of the different dimensions of the crater (diameter and depth), which would allow us to calculate more precise effusion rates.

7. References

Alle, 1983. Analysis of the eruptive history of the Volcán de Colima, Mexico (1560-1980). Geofísica Int.

Arámbula-Mendoza, R., Reyes-Dávila, G., Vargas-Bracamontes Dulce, M., González-Amezcua, M., Navarro-Ochoa, C., Martínez-Fierros, A., Ramírez-Vázquez, A., 2018. Seismic monitoring of effusive-explosive activity and large lava dome collapses during 2013–2015 at Volcán de Colima, Mexico. J. Volcanol. Geotherm. Res. 351, 75–88. https://doi.org/10.1016/j.jvolgeores.2017.12.017

Aries, S.E., Harris, A.J.L., Rothery, D.A., 2001. Remote infrared detection of the cessation of volcanic eruptions. Geophys. Res. Lett. 28, 1803–1806. https://doi.org/10.1029/2000GL012002

Ball, J.L., Calder, E.S., Hubbard, B.E., Bernstein, M.L., 2013. An assessment of hydrothermal alteration in the Santiaguito lava dome complex, Guatemala: Implications for dome collapse hazards. Bull. Volcanol. 75, 1–18. https://doi.org/10.1007/s00445-012-0676-z

Baloga, S., Pieri, D., 1986. Time-dependent profiles of lava flows. J. Geophys. Res. 91, 9543. https://doi.org/10.1029/jb091ib09p09543

Battaglia, M., Gottsmann, J., Carbone, D., Fernández, J., 2008. 4D volcano gravimetry. Geophysics 73. https://doi.org/10.1190/1.2977792

Belousov, A., Voight, B., Belousova, M., 2007. Directed blasts and blast-generated pyroclastic density currents: A comparison of the Bezymianny 1956, Mount St Helens 1980, and Soufrière Hills, Montserrat 1997 eruptions and deposits. Bull. Volcanol. 69, 701–740. https://doi.org/10.1007/s00445-006-0109-y

Calder, E.S., Lavallée, Y., Kendrick, J.E., Bernstein, M., 2015. Lava Dome Eruptions. Encycl. Volcanoes 343–362. https://doi.org/10.1016/B978-0-12-385938-9.00018-3

Calvari, S., Lodato, L., Spampinato, L., 2004. Monitoring active volcanoes using a handheld thermal camera. Thermosense XXVI 5405, 199. https://doi.org/10.1117/12.547497

Calvari, S., Lodato, L., Steffke, A., Cristaldi, A., Harris, A.J.L., Spampinato, L., Boschi, E., 2010. The 2007 stromboli eruption: Event chronology and effusion rates using thermal infrared data. J. Geophys. Res. Solid Earth 115, 1–20. https://doi.org/10.1029/2009JB006478

Campos-Enríquez, J.O., Alatorre-Zamora, M.A., 1998. Shallow crustal structure of the junction of the grabens of Chapala, Tepic-Zacoalco and Colima, Mexico. Geofis. Int. 37, 263–282.

Capra, L., Macías, J.L., Cortés, A., Dávila, N., Saucedo, R., Osorio-Ocampo, S., Arce, J.L., Gavilanes-Ruiz, J.C., Corona-Chávez, P., García-Sánchez, L., Sosa-Ceballos, G., Vázquez, R., 2016. Preliminary report on the July 10-11, 2015 eruption at Volcán de Colima: Pyroclastic density currents with exceptional runouts and volume. J. Volcanol. Geotherm. Res. 310, 39–49. https://doi.org/10.1016/j.jvolgeores.2015.11.022

Carn, S.A., 2015. Gas, Plume, and Thermal Monitoring. Encycl. Volcanoes 1125–1149. https://doi.org/10.1016/B978-0-12-385938-9.00065-1

Cashman, K. V., 1988. Crystallization of Mount St. Helens 1980-1986 dacite: A quantitative textural approach. Bull. Volcanol. 50, 194–209. https://doi.org/10.1007/BF01079682

CONAGUA, 2014. Precipitación a Nivel Nacional y por Entidad Federativa 2014, Servicio Meteorologico Nacional.

CONAGUA, 2013. Precipitación a Nivel Nacional y por Entidad Federativa 2013, Servicio Meteorologico Nacional.

Cortés, A., Garduño, V.H., Macías, J.L., Navarro-Ochoa, C., Komorowski, J.C., Saucedo, R., Gavilanes, J.C., 2010. Geologic mapping of the Colima volcanic complex (Mexico) and implications for hazard assessment. Spec. Pap. Geol. Soc. Am. 464, 249–264. https://doi.org/10.1130/2010.2464(12)

Fee, D., Matoza, R.S., 2013. An overview of volcano infrasound: From hawaiian to plinian, local to global. J. Volcanol. Geotherm. Res. 249, 123–139. https://doi.org/10.1016/j.jvolgeores.2012.09.002

Fougere, P.F., Tsacoyeanes, C.W., 1980. AFGL magnetometer observations of Mount St.

Helens eruption. Eos, Trans. Am. Geophys. Union 61, 1209–1210. https://doi.org/10.1029/EO061i050p01209-01

Garduño-Monroy, V.H., Saucedo-Girón, R., Jiménez, Z., Gavilanes-Ruiz, J.C., Cortés-Cortés, A., Uribe-Cifuentes, R.M., 1998. La falla tamazula, límite suroriental del bloque jalisco, y sus relaciones con el complejo volcánico de Colima, México. Rev. Mex. Ciencias Geol. 15, 132–144.

Garduño Monroy, V., Jiménez, Z., Gavilanes Ruiz, J., Cortés, A., Saucedo, R., Cifuentes, R., 1998. La falla Tamazula -límite suroriental del bloque Jalisco y sus relaciones con el complejo volcánico de Colima, México. Rev. Mex. ciencias geológicas, ISSN 1026-8774, Vol. 15, Nº. 2, 1998 15.

Geschwind, C.H., Rutherford, M.J., 1995. Crystallization of microlites during magma ascent: the fluid mechanics of 1980-1986 eruptions at Mount St Helens. Bull. Volcanol. 57, 356–370. https://doi.org/10.1007/BF00301293

Global Volcanism Program, 2017. Report on Colima (Mexico) (Crafford, A.E., and Venzke, E., eds.) [WWW Document]. Bull. Glob. Volcanism Network, 428. Smithson. Inst. https://doi.org/https://doi.org/10.5479/si.GVP.BGVN201708-341040

Global Volcanism Program, 2015. Report on Colima (Mexico) (Crafford, A.E., and Venzke, E., eds.) [WWW Document]. Bull. Glob. Volcanism Network, 4010. Smithson. Inst. URL https://volcano.si.edu/showreport.cfm?doi=10.5479/si.GVP.BGVN201510-341040 (accessed 1.24.20).

Gómez-Ortiz, D., Martín-Velázquez, S., Martín-Crespo, T., Márquez, A., Lillo, J., López, I., Carreño, F., 2006. Characterization of volcanic materials using ground penetrating radar: A case study at Teide volcano (Canary Islands, Spain). J. Appl. Geophys. 59, 63–78. https://doi.org/10.1016/j.jappgeo.2005.07.007

Gomez, C., 2006. Exposure to Volcanic Hazards , and Influence on Perception : A Case Study in Japan , Ten Years After the Unzen Fugendake Eruption. HAL, Arch. 1–26.

Gómez, H., 2019. Muon tomography using micromegas detectors: From Archaeology to nuclear safety applications. Nucl. Instruments Methods Phys. Res. Sect. A Accel. Spectrometers, Detect. Assoc. Equip. 936, 14–17.

https://doi.org/10.1016/j.nima.2018.10.011

Harnett, C.E., Thomas, M.E., Purvance, M.D., Neuberg, J., 2018. Using a discrete element approach to model lava dome emplacement and collapse. J. Volcanol. Geotherm. Res. 359, 68–77. https://doi.org/10.1016/j.jvolgeores.2018.06.017

Harris, A.J.L., Dehn, J., Calvari, S., 2007. Lava effusion rate definition and measurement: A review. Bull. Volcanol. 70, 1–22. https://doi.org/10.1007/s00445-007-0120-y

Harris, A.J.L., Murray, J.B., Aries, S.E., Davies, M.A., Flynn, L.P., Wooster, M.J., Wright, R., Rothery, D.A., 2000. Effusion rate trends at Etna and Krafla and their implications for eruptive mechanisms. J. Volcanol. Geotherm. Res. 102, 237–269. https://doi.org/10.1016/S0377-0273(00)00190-6

Hutchison, W., 2011. Growth and Thermal Evolution of an Andesitic Lava Dome Declaration of Authorship. Growth (Lakeland).

Hutchison, W., Varley, N., Pyle, D.M., Mather, T.A., Stevenson, J.A., 2013. Airborne thermal remote sensing of the volcán de colima (mexico) lava dome from 2007 to 2010. Geol. Soc. Spec. Publ. 380, 203–228. https://doi.org/10.1144/SP380.8

Jonathan H. Fink, 1990. Lava Flows and Domes. Springer-Verlag Berlin Heidelberg. https://doi.org/10.1007/978-3-642-74379-5

Komorowski, J.C., Jenkins, S., Baxter, P.J., Picquout, A., Lavigne, F., Charbonnier, S., Gertisser, R., Preece, K., Cholik, N., Budi-Santoso, A., Surono, 2013. Paroxysmal dome explosion during the Merapi 2010 eruption: Processes and facies relationships of associated high-energy pyroclastic density currents. J. Volcanol. Geotherm. Res. 261, 260–294. https://doi.org/10.1016/j.jvolgeores.2013.01.007

Korzhinsky, M.A., Botcharnikov, R.E., Tkachenko, S.I., Steinberg, G.S., 2002. Decade-long study of degassing at Kudriavy volcano, Iturup, Kurile Islands (1990-1999): Gas temperature and composition variations, and occurrence of 1999 phreatic eruption. Earth, Planets Sp. 54, 337–347. https://doi.org/10.1186/BF03353032

Luhr, J.F., Carmichael, I.S.E., 1980. The Colima Volcanic complex, Mexico. Contrib. to Mineral. Petrol. 71, 343–372. https://doi.org/10.1007/bf00374707.

Luhr, J.F., Carmichael, I.S.E., 1980. Contributions to Mineralogy and Petrology The Colima Volcanic Complex , Mexico Colinm 372, 343–372.

Luhr, J.F., Nelson, S.A., Allan, J.F., Carmichael, I.S.E., 1985. Active rifting in southwestern Mexico: Manifestations of an incipient eastward spreading-ridge jump. Geology 13, 54–57. https://doi.org/10.1130/0091-7613(1985)13<54:ARISMM>2.0.CO;2

Macías, J.L., Saucedo, R., Gavilanes, J.C., Varley, N., Velasco García, S., Bursik, M., Vargas Gutiérrez, V., Cortés, A., 2006. Flujos piroclásticos asociados a la actividad explosiva del Volcán de Colima y perspectivas futuras. Geos 25, 417–428.

Macías, J.L., Sosa-Ceballos, G., Arce, J.L., Gardner, J.E., Saucedo, R., Valdez-Moreno, G., 2017. Storage conditions and magma processes triggering the 1818 CE Plinian eruption of Volcán de Colima. J. Volcanol. Geotherm. Res. 340, 117–129. https://doi.org/10.1016/j.jvolgeores.2017.02.025

Maeno, F., Nakada, S., Yoshimoto, M., Shimano, T., Hokanishi, N., Zaennudin, A., Iguchi, M., 2019. A sequence of a plinian eruption preceded by dome destruction at Kelud volcano, Indonesia, on February 13, 2014, revealed from tephra fallout and pyroclastic density current deposits, Journal of Volcanology and Geothermal Research. Elsevier B.V. https://doi.org/10.1016/j.jvolgeores.2017.03.002

Murray, J.B., Stevens, N.F., 2000. New formulae for estimating lava flow volumes at Mt. Etna Volcano, Sicily. Bull. Volcanol. 61, 515–526. https://doi.org/10.1007/s004450050002

Nakada, S., Zaennudin, A., Yoshimoto, M., Maeno, F., Suzuki, Y., Hokanishi, N., Sasaki, H., Iguchi, M., Ohkura, T., Gunawan, H., Triastuty, H., 2016. Growth process of the lava dome/flow complex at Sinabung Volcano during 2013-2016. J. Volcanol. Geotherm. Res. https://doi.org/10.1016/j.jvolgeores.2017.06.012

Nakamura, S., Kikuchi, S., 1912. Permanent Magnetism of Volcanic Bombs. J-STAGE 6, 268–273. https://doi.org/https://doi.org/10.11429/ptmps1907.6.18_268

Navarro-Ochoa, C., Gavilanes-Ruíz, J.C., Cortés-Cortés, A., 2002. Movement and emplacement of lava flows at Volcán de Colima, México: November 1998-February 1999. J. Volcanol. Geotherm. Res. 117, 155–167. https://doi.org/10.1016/S0377-0273(02)00242-1

Norini, G., Capra, L., Groppelli, G., Agliardi, F., Pola, A., Cortes, A., 2010. Structural

architecture of the Colima Volcanic Complex. J. Geophys. Res. Solid Earth 115, 1–20. https://doi.org/10.1029/2010JB007649

Ogburn, S.E., Loughlin, S.C., Calder, E.S., 2015. The association of lava dome growth with major explosive activity (VEI ≥ 4): DomeHaz, a global dataset. Bull. Volcanol. 77. https://doi.org/10.1007/s00445-015-0919-x

Pallister, J.S., Diefenbach, A.K., Burton, W.C., Muñoz, J., Griswold, J.P., Lara, L.E., Lowenstern, J.B., Valenzuela, C.E., 2013. El domo riolítico del volcán Chaitén: secuencia eruptiva, tasa de emisión y fuente del magma riolítico. Andean Geol. 40, 277–294. https://doi.org/10.5027/andgeoV40n2-a06

Reyes-Dávila, G.A., Arámbula-Mendoza, R., Espinasa-Pereña, R., Pankhurst, M.J., Navarro-Ochoa, C., Savov, I., Vargas-Bracamontes, D.M., Cortés-Cortés, A., Gutiérrez-Martínez, C., Valdés-González, C., Domínguez-Reyes, T., González-Amezcua, M., Martínez-Fierros, A., Ramírez-Vázquez, C.A., Cárdenas-González, L., Castañeda-Bastida, E., Vázquez Espinoza de los Monteros, D.M., Nieto-Torres, A., Campion, R., Courtois, L., Lee, P.D., 2016. Volcán de Colima dome collapse of July, 2015 and associated pyroclastic density currents. J. Volcanol. Geotherm. Res. 320, 100–106. https://doi.org/10.1016/j.jvolgeores.2016.04.015

Ryan, G.A., Loughlin, S.C., James, M.R., Jones, L.D., Calder, E.S., Christopher, T., Strutt, M.H., Wadge, G., 2010. Growth of the lava dome and extrusion rates at Soufriére Hills Volcano, Montserrat, West Indies: 2005-2008. Geophys. Res. Lett. 37, 0–4. https://doi.org/10.1029/2009GL041477

Saucedo, R., Macías, J.L., Sheridan, M.F., Bursik, M.I., Komorowski, J.C., 2005. Modeling of pyroclastic flows of Colima Volcano, Mexico: Implications for hazard assessment. J. Volcanol. Geotherm. Res. 139, 103–115. https://doi.org/10.1016/j.jvolgeores.2004.06.019

Simmons, B., 2017. Frustum of a Cone or Pyramid [WWW Document]. Mathwords. URL https://www.mathwords.com/f/frustum.htm (accessed 1.9.20).

Sparks, R.S.J., Barclay, J., Calder, E.S., Herd, R.A., Komorowski, J.C., Luckett, R., Norton, G.E., Ritchie, L.J., Voight, B., Woods, A.W., 2002. Generation of a debris avalanche and violent pyroclastic density current on 26 December (Boxing Day) 1997 at Soufrière Hills Volcano, Montserrat. Geol. Soc. Mem. 21, 409–434.

https://doi.org/10.1144/GSL.MEM.2002.021.01.18

Sparks, R.S.J., Biggs, J., Neuberg, J.W., 2012. Monitoring volcanoes. Science (80-.). 335, 1310–1311. https://doi.org/10.1126/science.1219485

Sparks, R.S.J., Young, S.R., Barclay, J., Calder, E.S., Cole, P., Darroux, B., Davies, M.A., Druitt, T.H., Harford, C., Herd, R., James, M., Lejeune, A.M., Loughlin, S., Norton, G., Skerrit, G., Stasiuk, M. V., Stevens, N.S., Toothill, J., Wadge, G., Watts, R., 1998. Magma production and growth of the lava dome of the Soufriere Hills Volcano, Montserrat, West Indies: November 1995 to December 1997. Geophys. Res. Lett. 25, 3421–3424. https://doi.org/10.1029/98GL00639

Surono, Jousset, P., Pallister, J., Boichu, M., Buongiorno, M.F., Budisantoso, A., Costa, F., Andreastuti, S., Prata, F., Schneider, D., Clarisse, L., Humaida, H., Sumarti, S., Bignami, C., Griswold, J., Carn, S., Oppenheimer, C., Lavigne, F., 2012. The 2010 explosive eruption of Java's Merapi volcano-A "100-year" event. J. Volcanol. Geotherm. Res. 241–242, 121–135. https://doi.org/10.1016/j.jvolgeores.2012.06.018

Taran, Y., Gavilanes, J.C., Cortés, A., 2002. Chemical and isotopic composition of fumarolic gases and the SO 2 flux from Volcán de Colima, México, between the 1994 and 1998 eruptions. J. Volcanol. Geotherm. Res. 117, 105–119. https://doi.org/10.1016/S0377-0273(02)00239-1

Varley, N., 2016. Se forma nuevo domo en el Volcán de Colima [WWW Document]. Univ. Colima. URL https://www.ucol.mx/enterate/nota.php?docto=2473 (accessed 2.3.20).

Waitz, P., 1935. Datos históricos y bibliográficos acerca del Volcán de Colima. Memorias la Soc. Cient. bAntonio AlzateQ 53, 349–383.

Zobin, V.M., Arámbula, R., Bretón, M., Reyes, G., Plascencia, I., Navarro, C., Téllez, A., Campos, A., González, M., León, Z., Martínez, A., Ramírez, C., 2015. Dynamics of the January 2013–June 2014 explosive-effusive episode in the eruption of Volcán de Colima, México: insights from seismic and video monitoring. Bull. Volcanol. 77, 1–13. https://doi.org/10.1007/s00445-015-0917-z

Zorn, E.U., Le Corvec, N., Varley, N.R., Salzer, J.T., Walter, T.R., Navarro-Ochoa, C., Vargas-Bracamontes, D.M., Thiele, S.T., Arámbula Mendoza, R., 2019. Load stress controls on directional lava dome growth at volcán de Colima, Mexico. Front. Earth

Sci. 7, 1–18. https://doi.org/10.3389/feart.2019.00084